Route Optimization and Derivatization of the Antileishmanial Pentalinonsterol

Undergraduate Research Thesis

Presented in partial fulfillment of the requirements for graduation *with honors research distinction* in Chemistry in the undergraduate colleges of The Ohio State University

by

Andrew Clair Huntsman

The Ohio State University
May 2015

Thesis Defense Committee:

Professor James R. Fuchs, Department of Medicinal Chemistry (Project Advisor)
Professor Craig J. Forsyth, Department of Chemistry and Biochemistry (Co-Advisor)
Professor Randolph Roth, Department of History

Abstract

Leishmaniasis is a vector born disease identified by WHO as a globally neglected health problem. With 310 million people living at risk, there are an estimated 1.3 million new cases and 30-40 thousand deaths occurring annually. Current chemotherapeutics are limited by toxicity, cost, deliverability, patient compliance, and emergence of resistance. In an attempt to discover novel antileishmanials, the Kinghorn group isolated several biologically active compounds from the hexane extracts of the roots of *Pentalinon andrieuxii*. The roots have historically been used to alleviate skin ulcers formed by cutaneous leishmaniasis. Among the isolated compounds was pentalinonsterol which has proven to be a compelling new target molecule for the treatment of leishmaniasis. Synthetic preparation and route optimization of pentalinonsterol has facilitated further *in vitro* and *in vivo* studies as well as analogue synthesis for structure activity relationship (SAR) studies. An additional focus has been on 1) compound solubility, due to pentalinonsterol's highly lipophilic nature necessitating liposomal encapsulation for *in vivo* studies (the results of which have reinforced the enthusiasm for this natural product as a potential chemotherapeutic for leishmaniasis), and 2) development of probes to study mechanism of action. The analogues in development will provide a "handle" for the attachment of water soluble functional groups through a pro-drug approach and also facilitate the generation of conjugates for use as mechanistic probes. Our current strategy has focused on introducing this handle, a hydroxyl moiety, onto the core of pentalinonsterol as this approach is likely to withstand the most variability in functionality, an idea supported by preliminary SAR studies suggesting the importance of A-ring and C17 side chain functionalization for activity. Further studies will hopefully lead to the development of a new drug that is more cost effective, more potent and less toxic than current antileishmanial drugs.

Dedication

I would like to dedicate this thesis to my friends and family whose support has helped me throughout my undergraduate career.

Acknowledgements

I would like to acknowledge the Fuchs lab, our collaborators, and the funding that made this project possible:

Fuchs Group

Principal Investigator: Dr. James R. Fuchs

Members: Dr. Nivedita Jena, Dr. John Woodard, Dr. Pratiq Patel, Dr. Dalia Abdelhamid, Eric Schwartz, Chido Hambira, Janet Antwi, Tyler Wilson, Yara Mansour, Robert Demoret, and Malcolm Cole

Collaborators

Biological Testing: Dr. Satoskar (OSU, Medicine) and Dr. Parinandi (OSU, Medicine)

Encapsulation: Dr. Ainslie (UNC, Pharmacy)

Plant Extraction and Isolation: Dr. Kinghorn (OSU, Pharmacy)

Funding

NIH Grants AI 076309, AT 004160, 542 AI 090803 (to A.R.S.), RC4 AI 092624 (to A.R.S. and A.D.K.), DOD Grant W81XWH-14-2-0168 (to A.R.S.), College of Pharmacy Summer Undergraduate Research Fellowship, and College of Arts and Science Undergraduate Research Scholarship.

Vita

Poster Presentation at the 2014 Denman Undergraduate Research Forum

-1st Place prize in biological sciences-

Recipient of College of Pharmacy Summer Undergraduate Research Fellowship

Recipient of College of Arts and Sciences Undergraduate Research Scholarship

Poster Presentation at the 2015 Denman Undergraduate Research Forum

Poster Presentation at the 2015 College of Pharmacy Research Day

Publication pending….

Table of Contents

List of Figures

Chapter 1: Leishmaniasis

1.1 Parasitic Disease

Leishmaniasis is a protozoan parasitic disease transferred by the female *Phlebotomine* sand-fly vector.[1] Its lifecycle is outlined in **Figure 1.1** with two distinct life stages: promastigotes and amastigotes. The flagellated promastigote is transferred from vector to host during the blood meal of the sandfly (>1000 per bite[2]). Upon phagocytosis by the

Sandfly blood meal
Source: World Health Organization

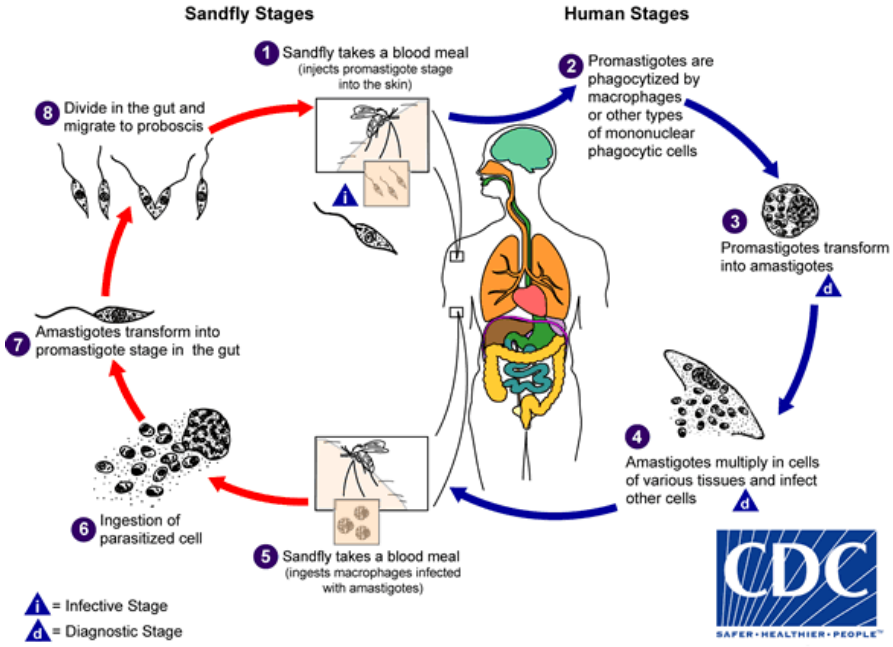

Figure 1.1. Leishmaniasis lifecycle.
Source: http://www.cdc.gov/parasites/leishmaniasis/biology.html

host's macrophages, promastigotes undergo transformation into the amastigote stage. Through binary fission they multiply and cause cell lysis, subsequently infecting other host macrophages. The lifecycle continues when a vector ingests a blood meal containing amastigote contaminated host macrophages. Transformation back into promastigotes and multiplication takes place within the vector to complete the cycle. Leishmaniasis is considered a zoonotic disease because it

requires a mammalian host reservoir to remain endemic to a region. No pathogenic response has been described for hosts other than dogs and humans.[2]

Clinical Manifestation	Leishmaniasis Species	Region of distribution
Cutaneous Leishmaniasis (oriental sore, tropical sore, uta ulcer, chiclero ulcer, or Aleppo boil)	*L. tropica*	Mediterranean countries, Afghanistan
	L. major	Middle East, Western and Northern Africa, Kenya
	L. aethiopica	Ethiopia
	L. mexicana	Central America, Amazon regions
Mucocutaneous Leishmaniasis (espundia)	*L. braziliensis*	Brazil, Peru, Ecuador, Columbia, Venezuela
Visceral Leishmaniais (kala-azar, dumdum fever, or black fever)	*L. donovani*	China, India, Iran, Sudan, Kenya, Ethiopia
	L. infantum	Mediterranean countries
	L. chagasi	Brazil, Columbia, Venezuela, Argentina

Figure 1.2. A variety of leishmaniasis species, their clinical manifestations, and affected regions.[3,4]

The resulting host infection is dependent on several factors including the parasite species and host immune response (which may contain the infection for weeks or even months before diagnostic abnormalities occur).[2] There are three clinical manifestations of leishmaniasis: cutaneous, mucocutaneous, and visceral leishmaniasis.[1] Cutaneous leishmaniasis (CL) is characterized by flat skin ulcers which feature slightly raised edges appearing on the host's exposed skin where bitten. These ulcers are known to leave disfiguring scars and cause disability. Visceral leishmaniasis (VL) is the deadliest clinical form of leishmaniasis. It causes inflammation/swelling of internal organs (typically the spleen, liver, and bone marrow) the results of which are often fatal if left untreated. Mucocutaneous leishmaniasis (ML) is less common than the other two and is characterized by the spread of infection to the mucous

membranes located around the ear, nose, and throat leaving the host mutilated. It is preventable by treatment of the original CL infection. Leishmaniasis species responsible for VL can thrive at core body temperatures (thus the internal organ infection) while those responsible for CL survive best at cooler peripheral temperatures (skin ulcers etc.).[2] These different manifestations, therefore, ultimately arise from localization due to the temperature dependence of various parasite species.

1.2 Demographics

According to information provided by the Center for Disease Control and Prevention (CDC) and the World Health Organization (WHO), there are 310 million people living at risk of leishmaniasis.[1] An estimated 1.3 million new cases and an upwards of 40 thousand deaths occur annually with approximately 12 million infected at any given time.[5] Figure **1.3**, A and B, contains information regarding the number of new cases of CL and VL, respectively, reported in the year 2012. The figure also provides a rough outline of endemic regions showing their location within primarily tropical climates. The numbers reported are likely underestimated due to the remoteness of poverty stricken locations afflicted by leishmaniasis and unreported cases of death by visceral leishmaniasis.[5] WHO has identified leishmaniasis as a globally neglected health problem due to the severe lack of information regarding incidents of the disease as well as the lack of funding and medical facilities for treatment in endemic regions.[1] The disease will spread with its vector, therefore more regions are at risk as global warming increases the range of the *phlebotomine* sandfly.[6] In immunosuppressed individuals, such as patients co-infected with HIV, leishmaniasis acts as an opportunistic disease further complicating treatment.[7]

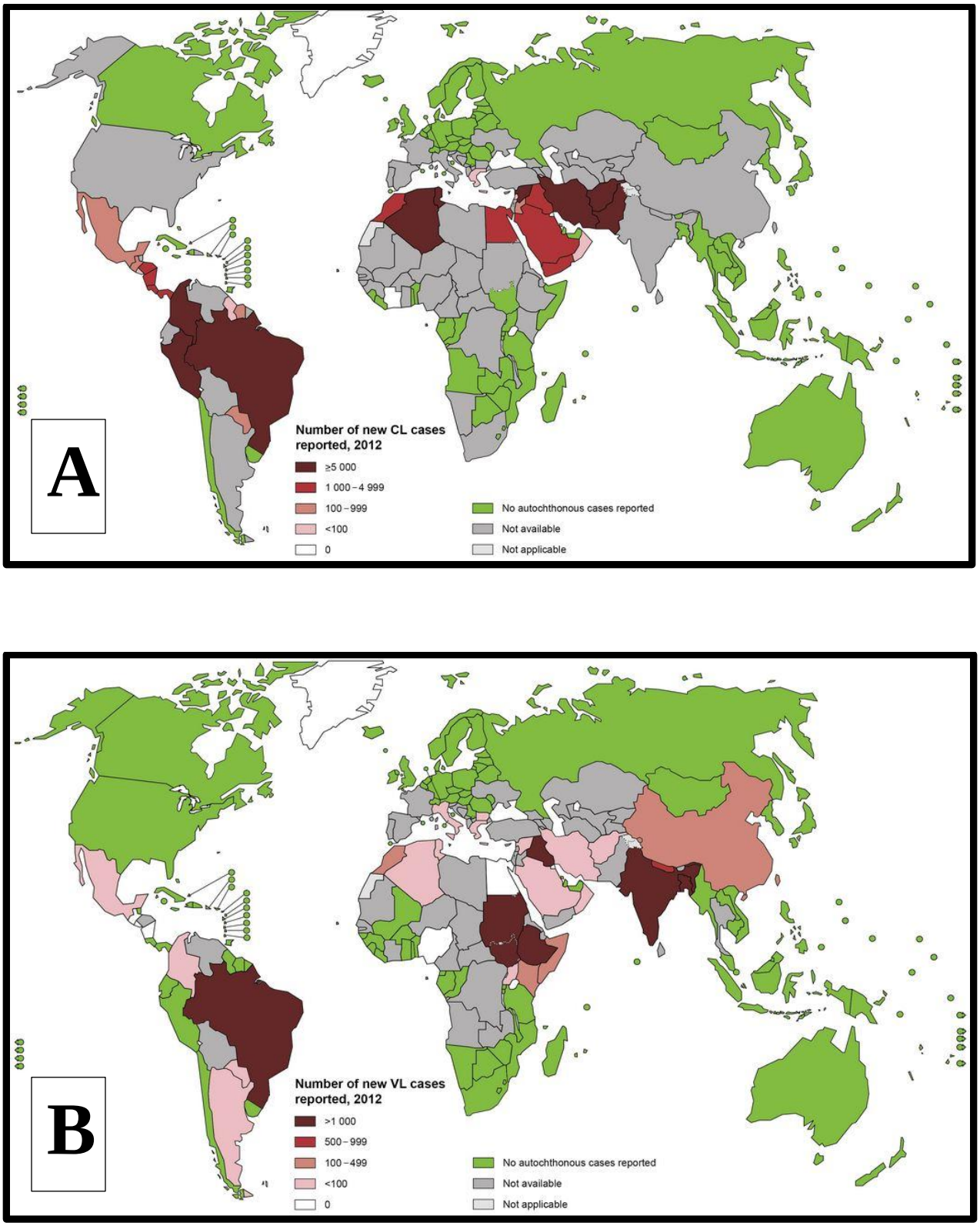

Figure 1.3. The number of new cases of CL (A) and VL (B) reported in 2012[1]

1.3 Current Antileishmanials

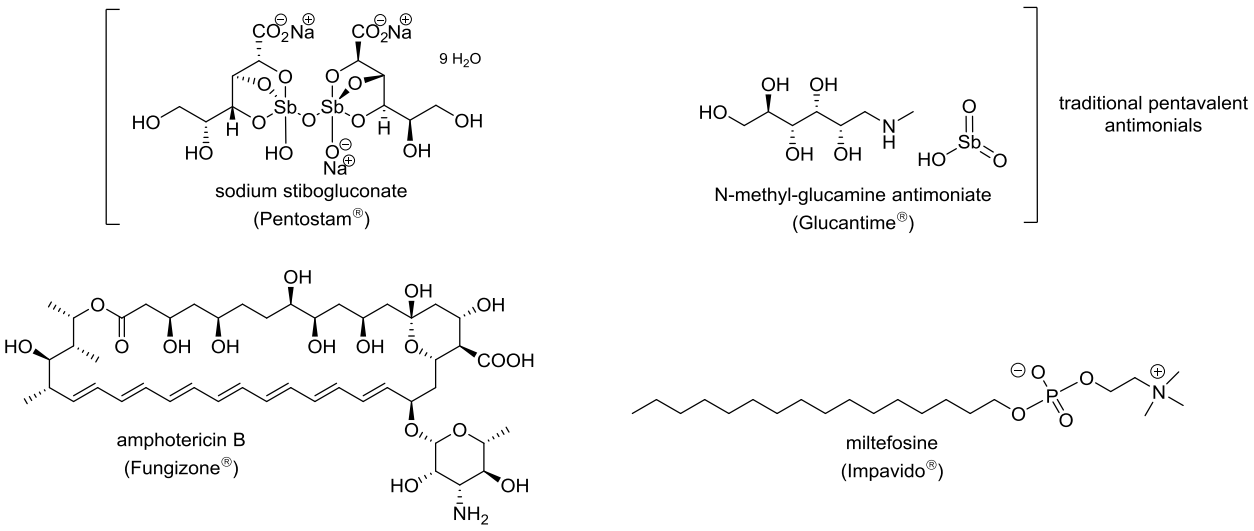

Figure 1.4. Current widely used chemotherapeutics for the treatment of leishmaniasis.[8]

Pentavalent antimonials have been the conventional chemotherapeutic regimen for over 75 years and remain the go-to drugs for the treatment of leishmaniasis around the world.[8] However, significant resistance (60% of VL patients in Bihar-India) has begun showing up since 1970 in both India and Sudan.[8] Other limitations of these antimonials include the need for intramuscular administration for up to 1 month long treatments and the severe cardiac, hepatic, pancreatic, and renal side effects associated with their use. Amphotericin B requires intravenous administration and is associated with renal toxicity, a problem that is reduced upon liposomal encapsulation, the cost of which drastically limits its practicality for use in undeveloped countries. Miltefosine is the first and still the only orally available treatment against leishmaniasis. Its side effects are mild compared to the other choices and it represents movement in the right direction for leishmaniasis treatments.

Each drug compound relies on target specificity which may only be effective against specific species of the leishmania parasite due to genetic differences. The existence of over 20

leishmania species makes it difficult to find a treatment that would be effective against all forms of the disease. Low patient compliance, due to administration methods and lack of proper healthcare systems, heightens the chance of resistance development in endemic regions. There is a high need for a diverse set of new treatments which address the concerns of high toxicity, high cost, and oral availability.

1.4 Methodology Introduction

Our approach to finding new potential antileishmanial chemotherapeutics is one based on collaborative efforts which require reciprocal communication. Bioassay guided fractionation is

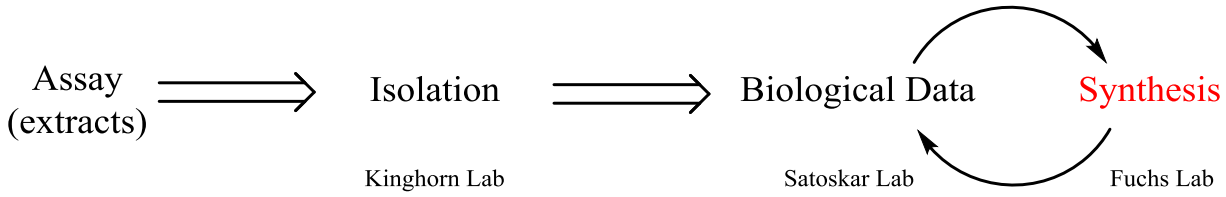

used to identify biologically active plant extracts. Following structure elucidation of isolated compounds, the biological activity of each individual compound is determined. Active isolates provide various leads for synthetic development which is generally required to facilitate more thorough biological studies of the parent molecule. A robust synthetic strategy then allows analogue development for structure activity relationship (SAR) and mechanism of action studies. The idea is that back and forth work/communication between the biology and chemistry labs will eventually lead to a selectively potent new chemotherapeutic.

While there exists a lot of potential for natural product antileishmanials as seen by various reports of active plant extracts, no natural products have yet to become available for the treatment of leishmaniasis.[8,9] Natural products present a source of compounds with structurally

unique scaffolds and non-precedented activities that could provide interesting leads for the treatment of leishmaniasis.

Chapter 2: Isolation and Preliminary Biological Studies of Pentalinonsterol

A collaboration between Dr. Douglas Kinghorn (natural product isolation chemistry - OSU), Dr. Abhay Satoskar (immunology and leishmaniasis - OSU), and Dr. James Fuchs (synthetic/medicinal chemistry - OSU) has provided a great opportunity for acquiring inspiration for antileishmanials from natural products. Of several plant species native to the Yucatan Peninsula of Mexico investigated for their antileishmanial properties, *Pentalinon andrieuxii* exhibited the most potential due to the observed activity of the crude extracts as well as its

Figure 2.1. Air dried roots of P. andrieuxii (Photo: Y. Deng)

reported use in the region. Interestingly, the roots of *P. andrieuxii* (found specifically in Campeche, Mexico) have been used in traditional Mayan medicine to treat CL lesions via daily cleansing of the wound with a root-based infusion followed by binding of the skin ulcer with the inner-root until visibly gone.[10,11]

Activity guided fractionation identified the hexane-soluble extract of the roots of *Pentalinon andrieuxii* as the most potent crude extract with an IC_{50} of 35 mg/mL against promastigotes of *L. mexicana*.[12] A topical application of the hexane *Pentalinon andrieuxii* root extract (PARE) were shown to visibly reduce the number of parasite containing macrophages present in the ear dermis of C57BL/6 mice infected with *L. mexicana*. **Figure 2.2** shows a decrease of infected macrophages upon treatment with PARE (left) as compared to the control (right) with the red

arrows pointing at examples of highly infected macrophages characterized by observable parasites (small black dots).

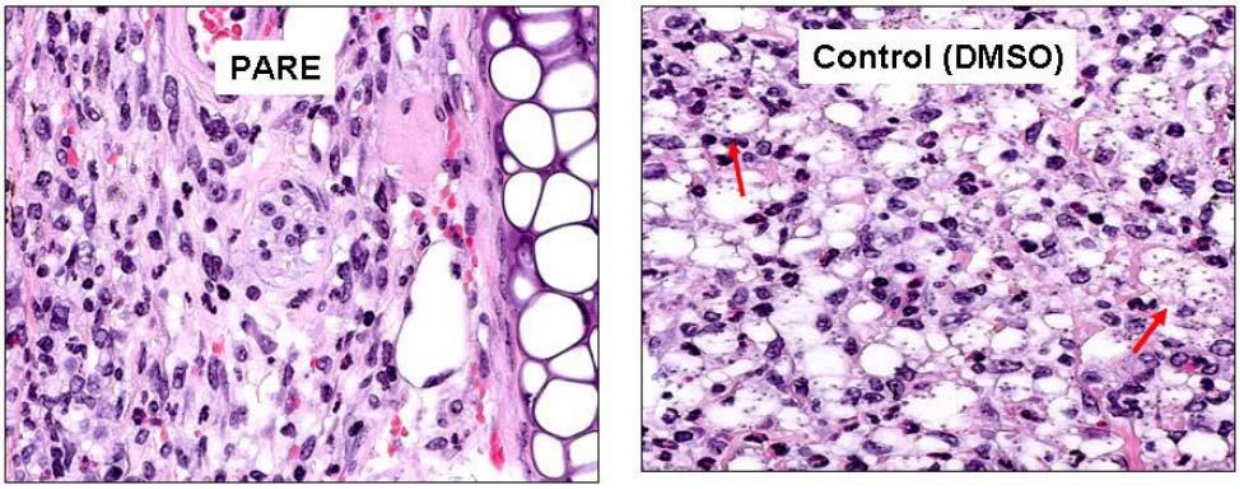

Figure 2.2. Stained sections of *L. mexicana* infected mouse ear following 21 days of application with a solution of 10 µg PARE dissolved in 50 µL of DMSO/PBS (unpublished work from the Satoskar lab).

Isolation and structure elucidation of the compounds contained within the hexane-soluble extract was accomplished in the Kinghorn Lab by Dr. Li Pan. Of the 20 compounds isolated from PARE (shown in **Figure 2.3**), biological evaluation determined the six outlined in red to be the most active. The active compounds can be split into three sterol structural classes:

I. A-ring α,β-unsaturated ketone

II. A-ring β,γ-unsaturated alcohol

III. D-ring α,β-unsaturated methyl ketone

Classes II and III have been pursued independently by other members in our lab. Oxidized cholesterol (**3**) belongs to the first class and exhibits nanomolar activity against *L. mexicana* amastigotes. However, it shows little potential for chemical optimization. The focus of this

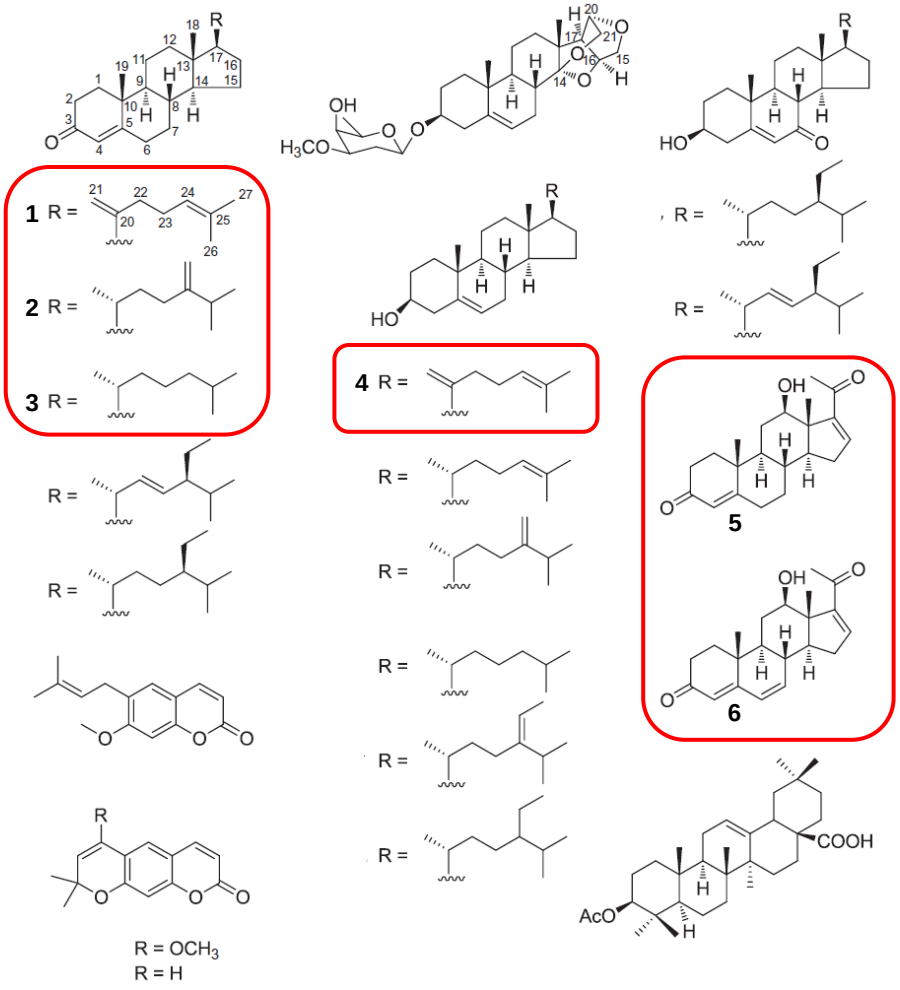

Figure 2.3. Compounds isolated from the hexane-soluble extract of *P. andrieuxii*

Compound	***L. mexicana*** **Promastigotes**	**Amastigotes**
pentalinonsterol (1)	**30.0**	**3.3**
2	**24.0**	**3.5**
3	**81.0**	**0.03**
4	**> 262**	**14.5**
dihydroneridienone (5)	**9.2**	**1.4**
neridienone (6)	**26.2**	**3.5**
Pentostam*	**346.1**	**2.7**

Figure 2.4. *In vitro* antileishmanial activity. IC_{50} values[12] in µM; anything greater than 100 µM is considered to be inactive which is the case for isolated compounds not listed in the figure. *Pentostam, also known as sodium stibogluconate, is an antimonial chemotherapeutic currently used for the treatment of leishmaniasis and was used as a reference standard in this experiment.

thesis is on the biologically active class I compound, pentalinonsterol (**1**), which represents a synthetically feasible novel target that offers a greater opportunity for optimization.

Pentalinonsterol (**1**) and compounds **2**, **3**, **5**, and **6** all possess the same A-ring oxidation state, which may contribute to their comparable IC_{50} values (**Figure 2.4**). Compound **4** lacks the same A-ring oxidation and yet was the only isolate besides **1**, **2**, **3**, **5**, and **6** that exhibited antileishmanial activity against amastigotes, albeit with lower relative potency. Closer inspection revealed that pentalinonsterol and compound **4** both have the same C17 side chain, possibly attributing this particular side chain to the activity of compound **4**. The absence of activity from compounds with extensively branched chains provides further evidence for the importance of this C17 chain. Thus, preliminary SAR investigation has identified the A-ring α,β-unsaturated ketone and the C17 side chain incorporating a prenyl group as the possible pharmacophore for the antileishmanial activity of pentalinonsterol (**1**).

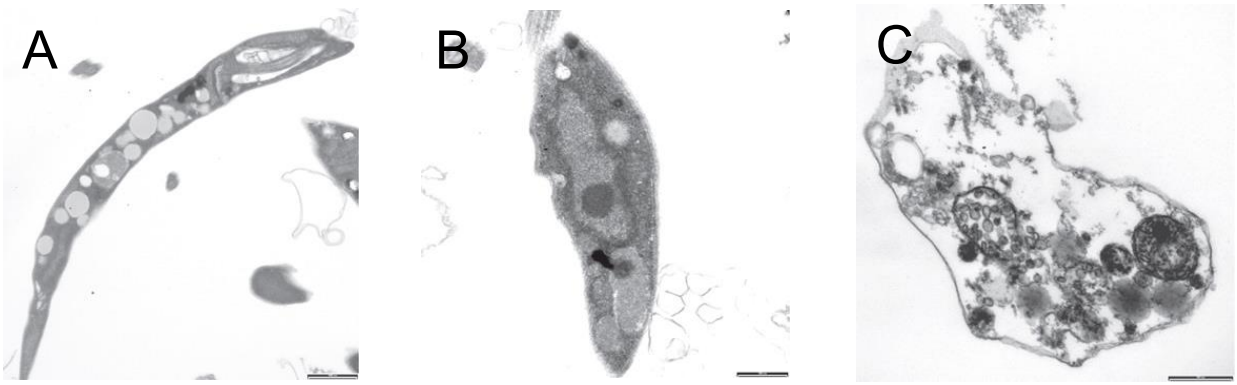

Figure 2.5. Electron microscopy of *L. mexicana* promastigotes.[12] A: untreated control; B: treated with pentostam (SSG-100 µM); C: treated with pentalinonsterol (100 µM)

Upon treatment with pentalinonsterol (**1**), parasitic promastigotes exhibited destructive membrane alterations (**Figure 2.5 - C**), more so than the reference sodium stibogluconate. *In vitro* activity against both promastigote and amastigote forms of the *L. mexicana* leishmania

parasite has proven the novel compound, pentalinonsterol (**1**), to be a potential new target molecule for the chemotherapeutic treatment of leishmaniasis. The desire for larger quantities (1.2 mg was isolated from 900 g of dried roots) to facilitate further biological studies led to the synthetic development of pentalinonsterol by our group.

Chapter 3: Synthesis of Pentalinonsterol and Structurally Similar Analogues

3.1 Synthetic Approach

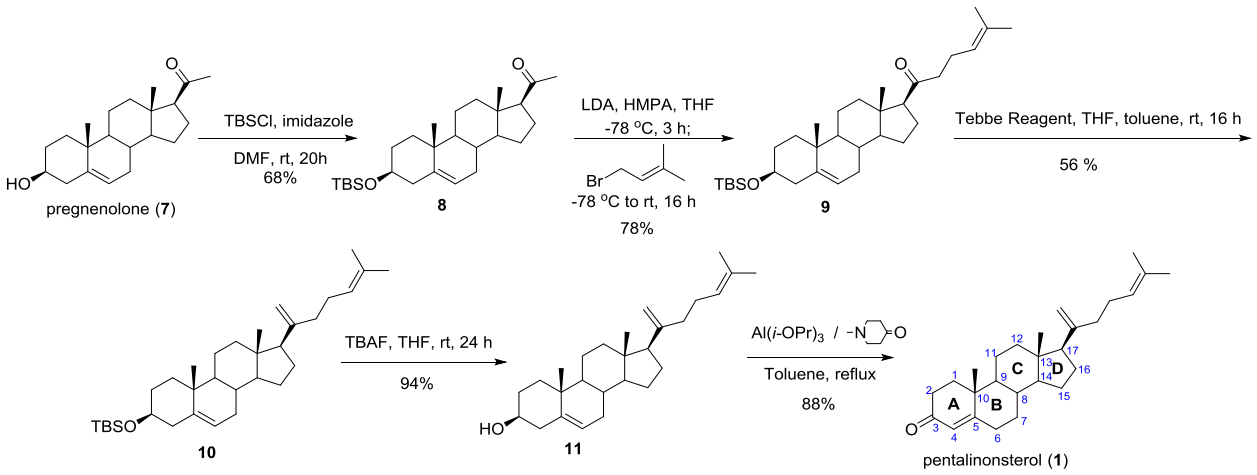

Figure 3.1. Dr. Abdelhamid's reaction scheme.[4]

The amount of natural product isolated from the dried roots of *Pentalinon andrieuxii* (1.2 mg from 900 g) limited the biological testing that could initially be performed on pentalinonsterol. As a novel chemical compound and one of the most active of the isolated sterols, it was considered an important synthetic target as additional material could facilitate thorough biological testing including structure activity relationship (SAR) and mechanism of action (MOA) studies. The synthesis of pentalinonsterol was initially achieved by Dr. Dalia Abdelhamid (**Figure 3.1**), a previous graduate student from the Fuchs lab, as part of her dissertation. The use of pregnenolone as the starting material allowed the semi-synthesis of pentalinonsterol in just five steps. First the A-ring alcohol was protected with a silyl group in order to limit reactivity of this position during the following steps. The C17 methyl ketone then provided quick access to the side chain via a key alkylation step which required an investigation of conditions. Dr. Abdelhamid worked out the conditions to afford an appreciable yield of 78% using the bulky base lithiumdiosoproplyamide (LDA) to favor kinetic enolate formation along with the charge separator hexamethylphosphoramide (HMPA) to make it more reactive towards the alkylating reagent. Initial failed attempts at acquiring the desired C18 methylene using the

Wittig reaction led to utilization of the Tebbe reagent for a 58% yield of the olefinated product. Deprotection of the A-ring protected alcohol proceeded in quantitative yield using tetrabutylammonium fluoride (TBAF) as the fluoride source. Implementation of the Oppenhauer oxidation as reported by Uskokovic *et al.* provided Dr. Abdelhamid with a mixture of tautomers indicating incomplete olefin isomerization following the alcohol oxidation.[13] Reich *et al.* previously reported the use of N-methylpiperidone instead of cyclohexanone as the hydride acceptor for the Oppenhauer oxidation of pregnenolone (the starting material for the pentalinonsterol synthesis).[14] Dr. Abdelhamid's use of N-methylpiperidone afforded pentalinonsterol from the β,γ–unsaturated alcohol in 88% yield.

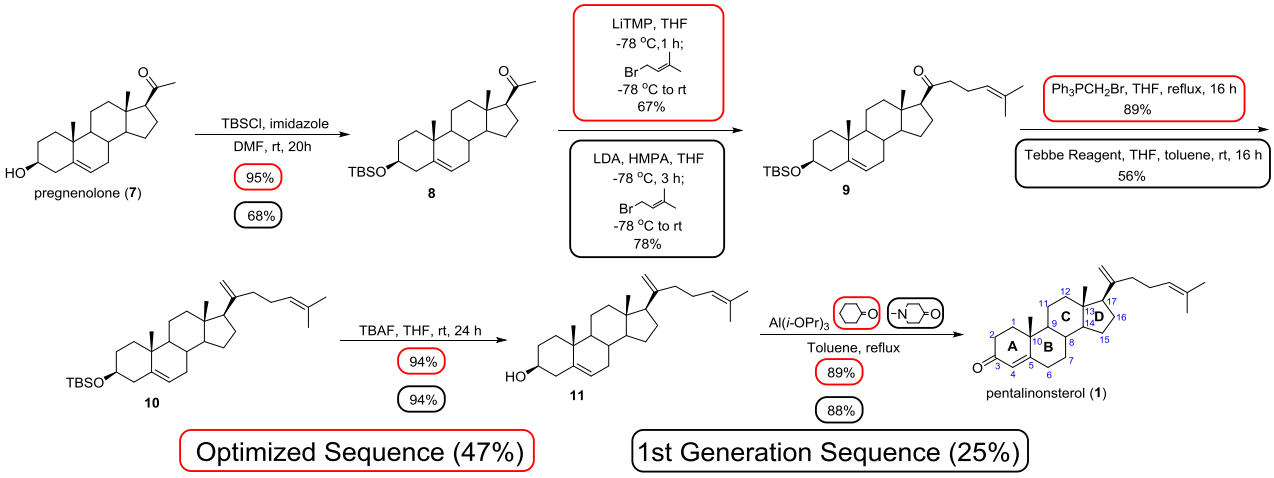

Figure 3.2. Optimized pentalinonsterol synthesis

While working towards multi-gram quantities of the product for additional biological studies, optimization of the synthetic sequence was performed during the summer of 2013. Minor changes were made to Dr. Abdelhamid's sequence which afforded an increased overall yield from twenty-five percent to forty-seven percent while decreasing the need for purification of intermediates and reagent cost. **Figure 3.2** displays an overlay of the optimized sequence

(outlined in red) with Dr. Abdelhamid's (outlined in black). Specific examples of optimization include:

- avoiding use of the carcinogenic charge separator HMPA in the alkylation
- co-isolation of mono- and di-alkylated product (to be resolved upon alcohol deprotection) due to separation complications following alkylation
- successful implementation of Wittig olefination over the more expensive Tebbe reagent
- hexane trituration of olefination product
- successful Oppenhauer oxidation with subsequent tautomerization using cyclohexanone rather than the more expensive N-methylpiperidone as the hydride acceptor

Wanting to avoid the use of carcinogenic HMPA led to the use of lithium tetramethylpiperidide (LiTMP) over LDA for kinetic enolate formation. Although pure materials were isolated at this stage for yield determination, it was demonstrated that co-isolation of both mono- and di-alkylated products (requiring less time and smaller quantities of solvent) generated in the alkylation reaction could efficiently be carried through the olefination step and deprotection reaction with an increase in overall yield since material was typically lost during purification. The increased polarity of the compounds upon deprotection of the silyl protected alcohol made "late-stage" separation of these products much easier. In the olefination step, excess Wittig reagent (approximately 10 equivalents) was found to afford a good yield, both giving more product and costing less than materials required for the Tebbe methylenation. Following quantitative deprotection of the silyl protected alcohol, an Oppenhauer oxidation was utilized to introduce the A ring oxidation state. The use of cyclohexanone as a cheaper alternative to N-methylpiperidone afforded us the α,β-unsaturated ketone as the only isomer in similar yields to Dr. Abdelhamid. N-methylpiperidone was reported by Reich *et al.* as an easily extractable

(water soluble upon protonation) alternative to excess cyclohexanone in the reaction mixture.[14] However, in this case there was no trouble in isolating pentalinonsterol from cyclohexanone using conventional flash chromatography. The complete isomerization to the α,β-unsaturated ketone is believed to be the thermodynamic result of extended reaction times.

Having facilitated further biological studies of pentalinonsterol through the preparation of gram quantities of the natural product, interest in the compound shifted toward production of analogues of this natural product in an effort to explore and improve its pharmacological properties. This first round of analogues focused on the importance of the predetermined pharmacophore. A-ring analogues **12** and **13** were acquired through the post-synthetic manipulation of pentalinonsterol. A Luche reduction of the C3 ketone yielded both epimers of

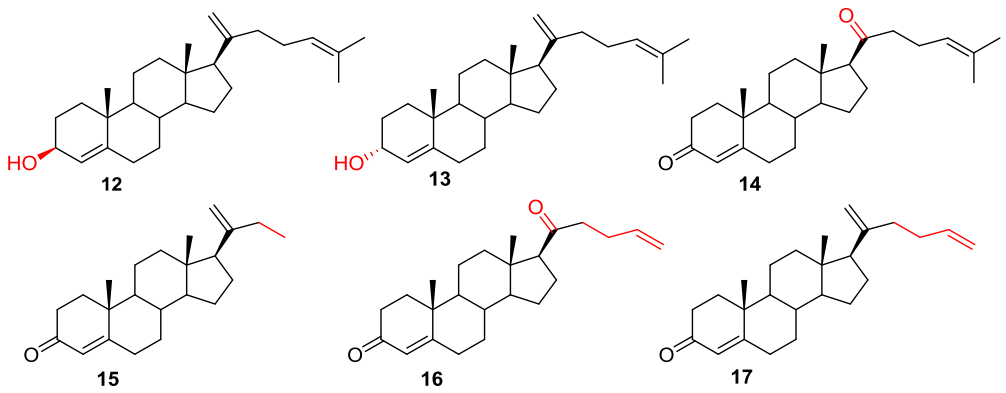

Figure 3.3. Library of analogues to date.

the resulting allyl alcohol while a DDQ oxidation yielded the oxidized 1,4-dienone product of pentalinonsterol (not shown) which proved to be unstable. The rationale behind these analogues was to probe the true importance of the A-ring oxidation state via changes in polarity and hydrogen bond donor/acceptor capabilities which have an impact on binding interactions and drug properties. Variation of the alkylating reagent in the synthetic sequence en route to pentalinonsterol led to C17 side chain analogues while omission of the Wittig olefination led to

C18 ketone analogues of pentalinonsterol. The rationale behind these C17 side chain analogues (**15-17** prepared by Robert Demoret) is to probe the importance of the length, substitution, and oxidation state of this chain as this might affect binding within a particular enzyme pocket.

3.2 Biological Studies Facilitated by Synthetic Production of Pentalinonsterol

Promising results have been obtained from *in vivo* and *in vitro* studies of synthetically prepared pentalinonsterol (PEN) suggesting that its activity can be attributed to multiple mechanisms of action. In collaboration with the Ainslie and Satoskar labs, *in vivo* results with

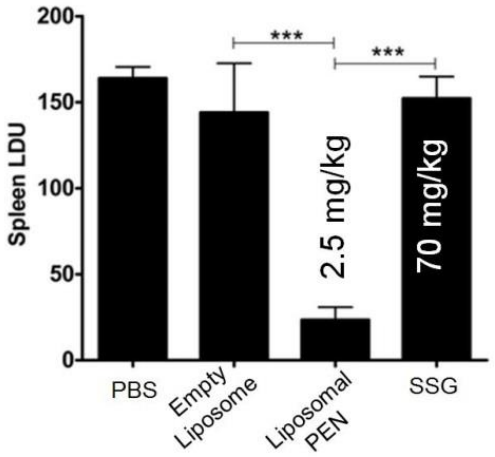

Figure 3.4. *In vivo* results following treatment of *L. donovani* infected mice with encapsulated pentalinonsterol (encapsulation by the Ainslie Lab).[15]

encapsulated PEN revealed amastigote load reduction in the spleen (**Figure 3.4** - 83% reduction), liver (64%), and bone marrow (57%) of mouse hosts with respect to an empty liposome control. Comparatively, a conventional chemotherapeutic sodium stibogluconate (SSG) showed low clearance at a 28 times greater concentration. Bone marrow amastigote reduction is key to eradication of VL due to its ability to act as a parasite reservoir. Elevated levels of ALT and AST liver enzymes induce cell necrosis and thus represent markers for cytotoxicity of

compounds.[16] Levels of these enzymes relative to control suggest that encapsulated PEN was well tolerated by the mice.[17] An MTT assay performed with non-encapsulated pentalinonsterol also showed high cell viability and therefore low toxicity associated with doses of 25 and 50 µM.

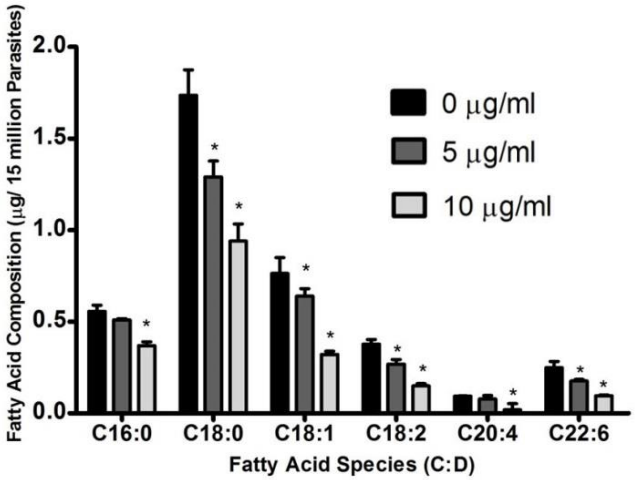

Figure 3.5. Fatty acid composition of *L. donovani* promastigotes after treatment with PEN (Parinandi Lab).[15]

In studies on pentalinonsterol, carried out in the Parinandi lab, a dose-dependent decrease in fatty acid composition of *L. donovani* promastigotes was observed (**Figure 3.5**), suggesting that some of PEN's activity is attributed to the breakdown of phospholipids in the parasite's membrane - possibly through activation of phospholipases A1 and A2. Physical evidence of this mechanism of action was seen previously during preliminary *in vitro* studies where alterations to a promastigote membrane were seen following treatment with pentalinonsterol (**Figure 2.5**). Minimal discrepancy in fatty acid composition suggests pentalinonsterol's potential for efficacy against multiple species.

An observed increase in mature and parasite free hepatic granuloma following treatment with encapsulated pentalinonsterol as well as increased T cell proliferation indicate an induced host immune response via increase in IFN-γ and IL-12 release. Formation of mature hepatic

granulomas as a result of increased IFN-γ release has previously been shown to contribute to reduction of amastigotes within the host, while in general increased IFN-γ and IL-12 release has been associated with various anti-parasitic immune responses including the observed formation of mature hepatic granuloma.[18,19,20,21]

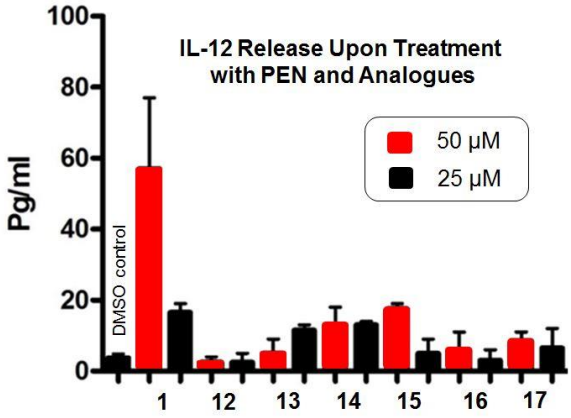

Figure 3.6. PEN and structurally related analogues effect on IL-12 release from bone marrow dendritic cells as measured by ELISA (Satoskar Lab; red bars added for clarity).

The observed pro-inflammatory cytokine response presented the idea of PEN as an adjuvant which prompted biological testing to determine how **Figure 3.3** analogues (*in vivo* load reduction studies currently underway) affect IL-12 (**Figure 3.6**) and IL-10 (data not shown) release. IL-10 levels were relative to the control for all compounds tested, thus demonstrating that this system does not promote an anti-inflammatory response. Pentalinonsterol is the most potent at promoting IL-12 release compared to its structural analogues to date, reinforcing the importance of the A-ring oxidation state and the C17 side chain. However, improvement of its drug properties is required for consideration as an effective antileishmanial. Pentalinonsterol's lipophilic nature makes it difficult to introduce into a biological system without encapsulation which introduces an increased cost of production and requires intravenous administration.

Chapter 4: Hydroxyl Containing Analogues of Pentalinonsterol for Solubility Improvement and Mechanism of Action Studies

4.1 Addressing Solubility Issues

Pentalinonsterol is a very lipophilic molecule (logP = 6.29, ChemBioDraw Ultra version 14.0) which limits its water solubility, thus limiting its absorption into and transport throughout a biological system. In medicinal chemistry, efforts are often made to attach polar functional groups onto a potential drug molecule to optimize drug properties and make drug delivery more feasible. As shown previously, liposomal encapsulation facilitated *in vivo* studies of pentalinonsterol but required intravenous administration. The ideal medication can be taken orally, requiring no trained medical attendants while simultaneously improving patient compliance. The goal of this portion of the project, therefore, is to modify the existing synthetic route to pentalinonsterol by utilizing strategies employed in previous sterol syntheses to "install" a functionalizable hydroxyl group onto the core of pentalinonsterol in the hopes of increasing its water solubility using a pro-drug approach. As noted above, it appears that the C17 side chain and the α,β-unsaturated ketone on the A ring are necessary for the biological activity of pentalinonsterol. Therefore, the proposed synthesis is focused on introducing a hydroxyl group onto the core ring system of pentalinonsterol which would be expected to tolerate more variability in functionality.

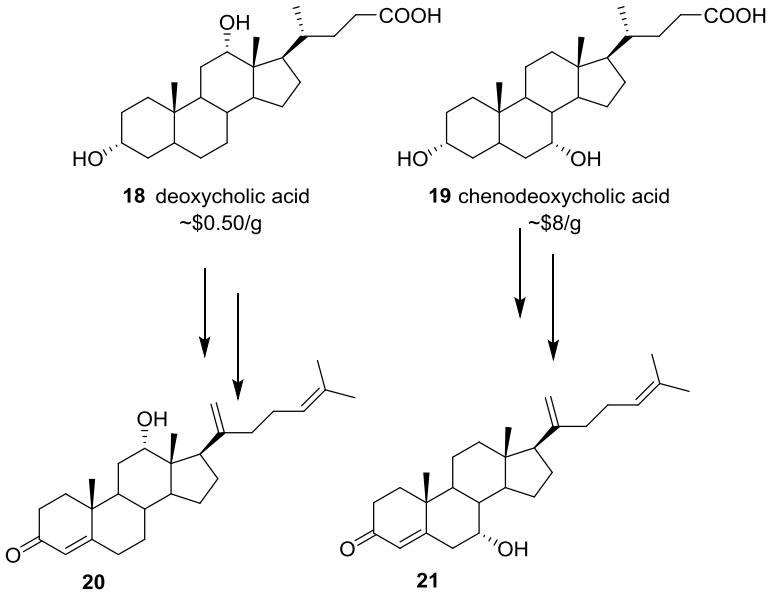

Figure 4.1. Desired analogues

C12 and C7 are practical positions for the introduction of a hydroxyl group because of the choice of starting material. Pregnenolone was the obvious starting material choice for the synthesis of pentalinonsterol as it could be transformed into the product in five simple organic reactions. The desired hydroxyl installment, however, cannot easily be accomplished on the sterol backbone of pregnenolone. Deoxycholic acid (C12 hydroxyl) and chenodeoxycholic acid (C7 hydroxyl), naturally occurring bile acids structurally related to cholic acid, are commercially available starting materials that conveniently already possess a hydroxyl group at either of the two desired positions. Because the newly introduced hydroxyl group may have an adverse effect on compound activity, assembling both regioisomeric analogues increases the probability that one will retain or exhibit improved activity. The presence of a hydroxyl group should facilitate further functionalization of the molecule in order to improve solubility or prepare molecular probes.

4.2 Analogue Development Methodology

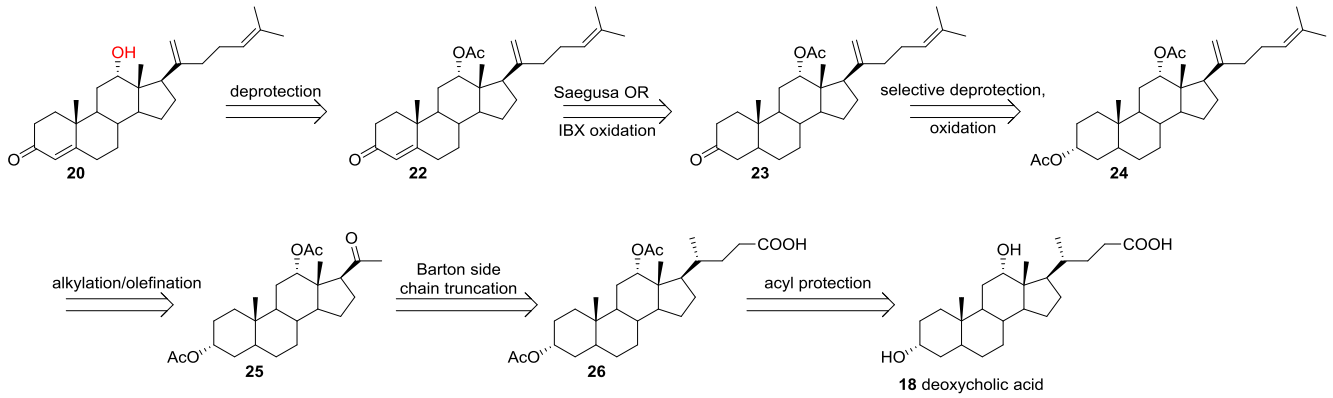

Figure 4.2. Retrosynthetic analysis of hydroxyl-pentalinonsterol analogues. Reaction sequences were expected to be tolerated equally well by both deoxycholic and chenodeoxycholic acid.

Although cholic acid derivatives provide a unique starting material for the synthesis of these hydroxyl containing pentalinonsterol analogues, their synthesis is not trivial. There is precedence by Barton *et al.* for the three step truncation of bile acid side chains to the methyl ketone in the presence of acetate protected alcohols on molecular systems very similar to both deoxycholic acid and chenodeoxycholic acid.[22] At that stage, methodology similar to that reported by Dr. Abdelhamid/later optimized could be applied to introduce the required side chain functionality.[4] The next complication arises with respect to incorporation of the α,β-unsaturated ketone. This requires a selective deprotection of the C3 hydroxyl substituent, reported on a similar system using acetate protecting groups by Geoffroy *et al*, followed by an oxidation to give the C3 ketone.[23] The presence of the ketone moiety sets up the molecule for an IBX oxidation based on literature precedent which our lab has previously demonstrated, affording the final product after a simple deprotection of the C12 or C7 hydroxyl group.[24,25]

4.3 Progress, to Date, Towards Hydroxyl Containing Analogues

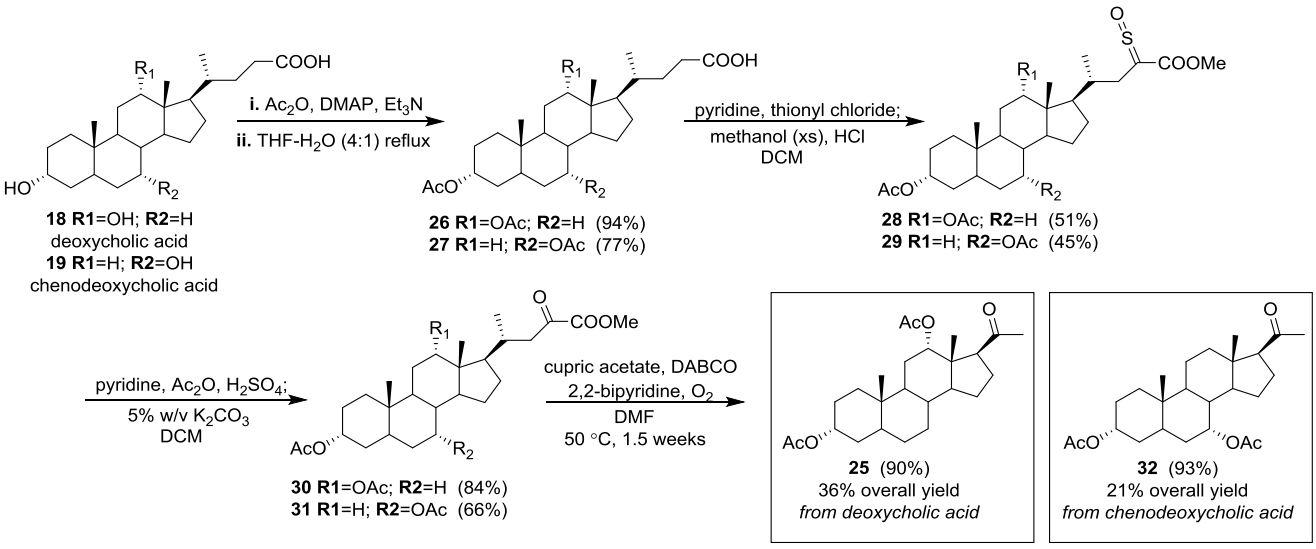

Figure 4.3. Our use of the Barton side chain truncation sequence on deoxycholic and chenodeoxycholic acid.

The Barton *et al.* side chain truncation reaction sequence undergoes several unique mechanistic transformations. Thionyl chloride is used to install a sulphine group alpha to an ester followed by conversion to α-ketoester **30**/**31** which when treated with cupric acetate in the presence of atmospheric oxygen undergoes a three carbon truncation with the liberation of 2 moles of carbon monoxide and 1 mol of carbon dioxide.[22] Some drawbacks to the Barton side chain truncation are the low yielding sulfonation transformation when performed on our system as well as the 1.5 week reaction time for the conversion of **30**/**31** to **25**/**32**. Despite these drawbacks, this sequence has provided enough material to move forward with the synthesis of our hydroxyl-containing analogues. Further optimization will be performed if one or more of the analogues require substantial biological investigation following initial studies.

Attempting the alkylation on compound **32** afforded six new spots by thin layer chromatography (TLC) indicating possible alkylation of the acetate protecting groups in addition to alkylation at the C17 methyl ketone. Our previous synthesis of pentalinonsterol showed that the alkylation could be carried out in good yields in the presence of silyl ether protecting groups. Having determined that the side chain degradation cannot be performed in the presence of silyl protecting groups due to the acidic conditions required, the acetate protecting groups were exchanged for silyl ether protecting groups after obtaining the key methyl ketone intermediate.

The alkylation of protected methyl ketone **35** (**Figure 4.4**) has been successfully performed on 30 mg scale to obtain mono- and di-alkylated products as noted by crude NMR. The crude alkylation products were then subjected to Wittig conditions as described previously in the synthetic route to pentalinonsterol. The products of the reaction have not yet been isolated and interpretation of the crude NMR has not been conclusive. It will be necessary to synthesize

larger quantities of compounds **25** and **32** to facilitate obtaining these intermediates in higher yields and allow further investigation of these reactions.

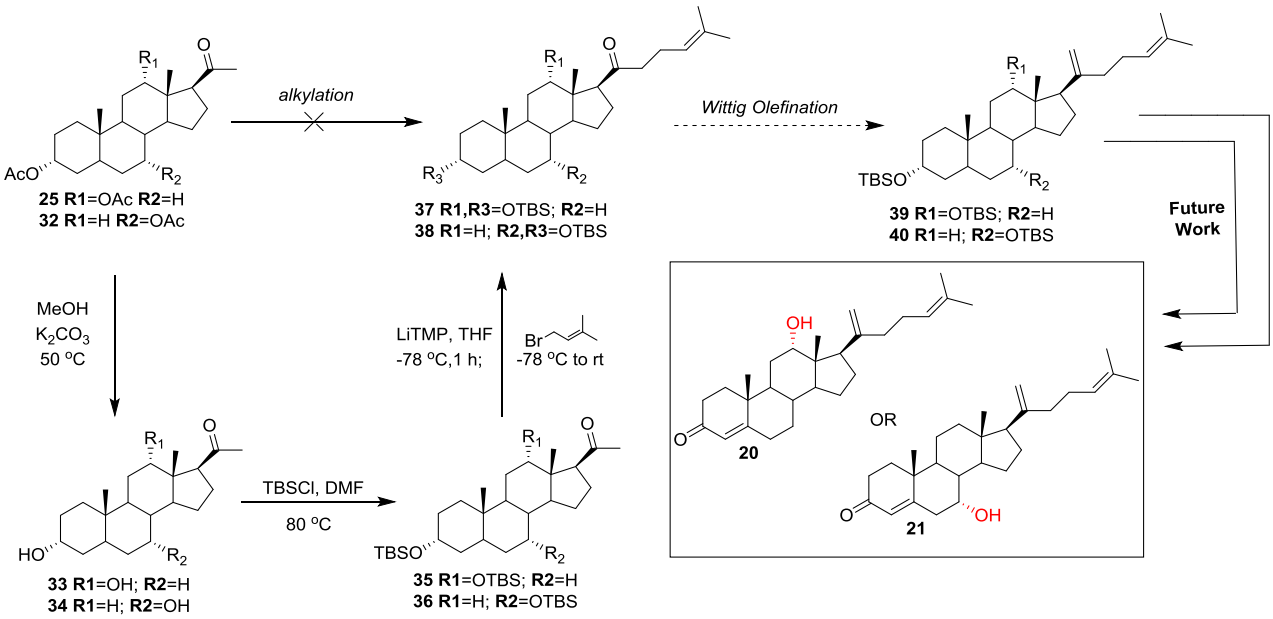

Figure 4.4. Incorporation of pentalinonsterol synthesis

4.4 Remaining Steps towards Hydroxyl Containing Analogues

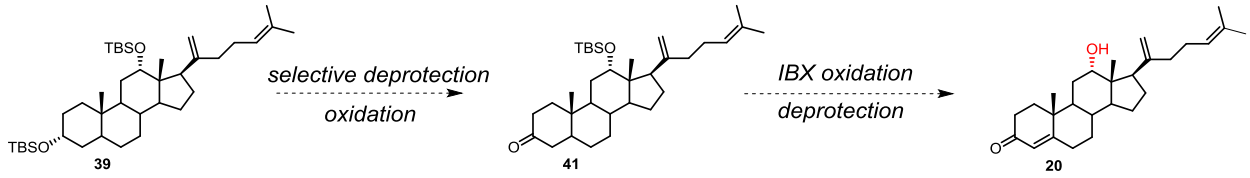

Figure 4.5. Remaining synthetic transformations.

Incorporation of the A-ring α,β–unsaturated ketone will require some additional synthetic transformations. We initially found precedence for the selective removal of the A-ring over the C-ring protecting group acetates.[23] The acetate/silyl exchange of protecting groups brought on

the question of whether or not selective deprotection of the silyl group was plausible. The secondary neopentyl C12 alcohol has proven to be a difficult steric obstacle for installing protecting groups as seen by the harsher conditions required for silyl protection. Thus we were not surprised to find precedence for the selective deprotection of silyl groups as well. A patent by O'Doherty *et al*. reports selective removal of the A-ring silyl protecting group over the C-ring.[26] There is no reported precedent, however, for similar selectivity over the B-ring hydroxyl present in the chenodeoxycholic derived hydroxyl analogue. If the same reaction conditions do not selectively remove the A-ring and instead results in deprotection of both alcohols, we will follow the regioselective oxidation as reported by Li *et al.* to selectively install the C3 ketone following complete deprotection.[27] IBX oxidation will then be utilized to afford the desired A-ring oxidation state.[25]

4.5 Final Analogues for Solubility and MOA Studies

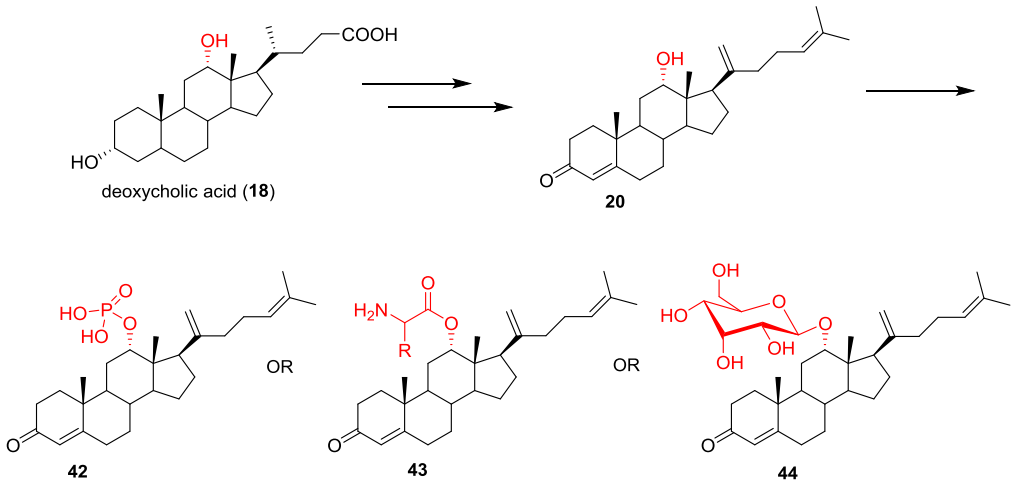

Figure 4.6. Possible choices for prodrugs.

There are multiple options for increasing the water solubility of the desired hydroxyl-analogues. Our group has previously explored the use of phosphate groups as prodrug conjugates on unrelated projects, but other possibilities (**Figure 4.6**) include amino acids, carbohydrates, and succinates (not shown). Dextran polymers as prodrugs have been investigated and accumulation selectivity depending on molecular weight of the dextran polymer conjugate has been reported.[28,29] Zhang and Mehvar report liver and spleen target specificity using the dextran-70 prodrug of methylprednisolone (an immunosuppressive sterol used to prevent organ transplant rejection).[30] Their rationale was to target the site of action, liver and spleen, which are two organs we wish to target due to accumulation of amastigotes in these organs with visceral leishmaniasis. **Figure 4.7** shows what the hydroxyl-analogue looks like with this prodrug compared to the methylprednisolone prodrug.

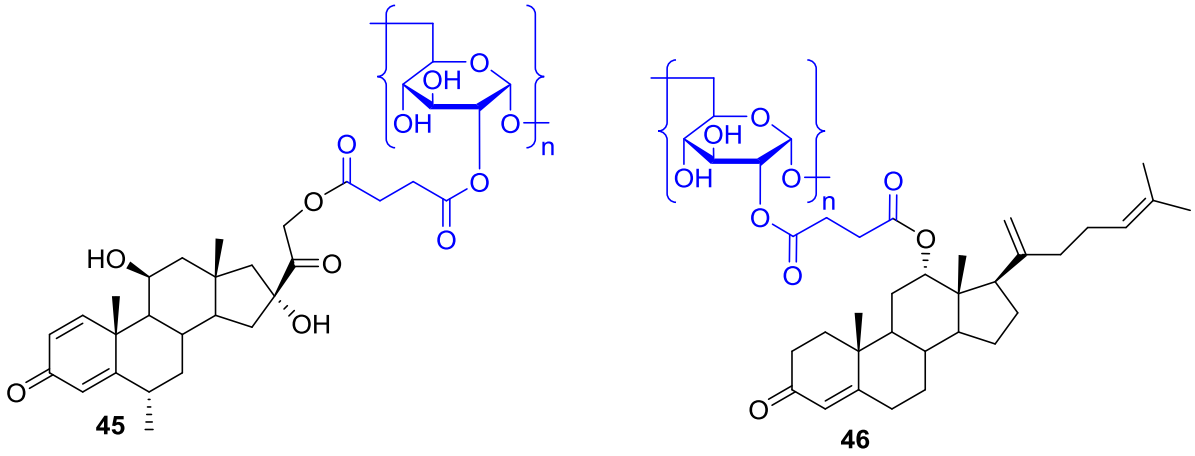

Figure 4.7. Prodrug approach modelling work done by Zhang and Mehvar to target liver and spleen with the hopes of improving bioavailability as well.

Multiple syntheses of dextran macromolecule prodrugs have been reported with minor alterations over time using carbonyldiimidazole (CDI) for attaching the drug molecule to dextran-70 via the carboxylic acid substituents on either side of a succinate linker.[31,32] Some

complications may arise due to the steric hindrance previously associated with the C12 hydroxyl analogue and so attachment at the C7 position might be more plausible. Regardless, this prodrug approach represents a very interesting route towards improving not only solubility but delivery specificity as well.

The introduction of a hydroxyl group onto the sterol backbone could be employed not only for the purposes of increasing solubility, but also to probe the mechanism of action of these compounds through linkage of the sterol to an affinity or fluorescent probe. **Figure 4.8** depicts the attachment of biotin to the C7 hydroxyl PEN analogue. A review by Katja Hubel, Toben

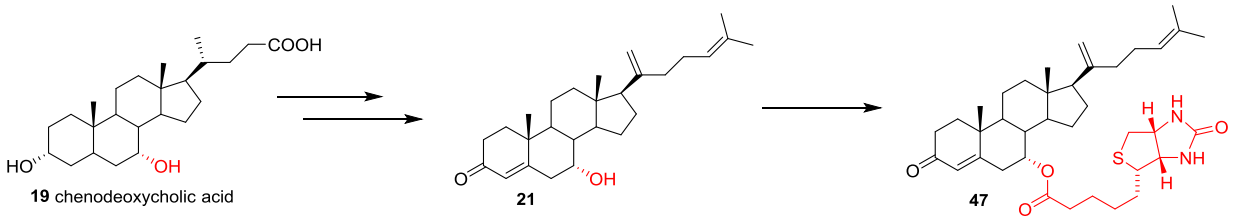

Figure 4.8. Hydroxyl-containing analogue as a mechanistic probe.

LeBmann, and Herbert Waldmann discusses use of biotin as a small molecule mechanistic probe.[33] Following attachment, the analogue can be immobilized on beads covalently bound to streptavidin for which biotin has a high affinity. A test cell is then lysed and combined with the immobilized small molecule in various pull down assays to identify the small molecule's target protein(s). A fluorescent attachment to the linker could facilitate easier identification of target proteins.

Several examples of affinity based target protein identification experiments which could utilize a bead bound bioactive small molecule as depicted in Figure 4.9 are discussed in a review by Amanda McFedries, Adam Schwaid, and Alan Saghatelian.[34] A particularly interesting experiment involved culturing "heavy" cells in media containing isotopic amino acids which end

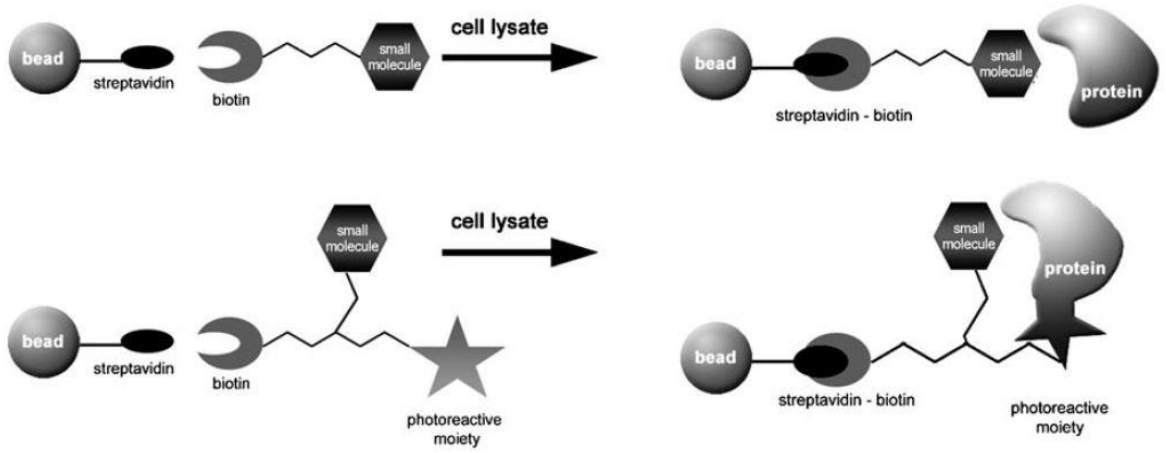

Figure 4.9. Pull down assay experiment[33]

up incorporated in cell's protein. The same proteins with lower mass are present in "light" cells. Lysates of both are incubated with the beads except that prior to incubation the light cell lysate is treated with a soluble form of the same small molecule which is attached to the bead to prevent attachment to the bead. Bound proteins are eluted from the beads and combined following the removal of lysate. The target proteins are then identified by increased ratio of heavy protein to light protein using quantitative proteomics.[35,36]

Successful use of coumarin analogues as fluorescent probes for natural products has been investigated by J. J. La Clair.[37] The coumarin analogues were selected based on their ability to leave original activity and delivery unaffected. Analogues **49** and **50**, whose syntheses from compound **48** are outlined in the article, could be utilized with our prepared conjugates which contain hydroxyl handles for attachment via Mitsunobu or aziridine ring-opening as depicted in **Figure 4.10**. LED fluorescence microscopy could then be used to identify localization of our compound.

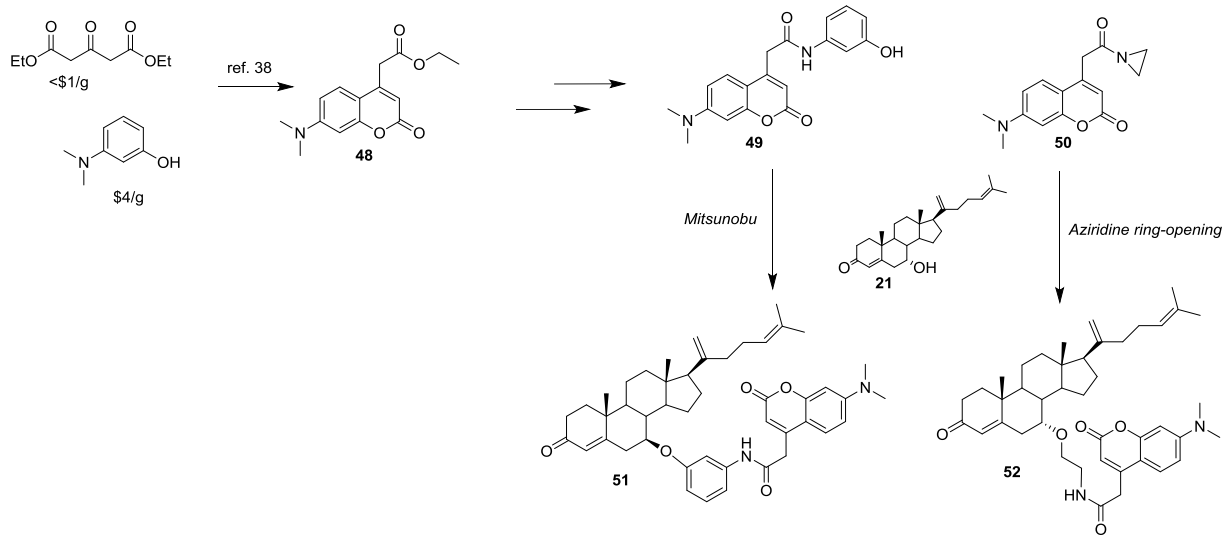

Figure 4.10. Two proposed mechanistic probes inspired by work on reported natural product mechanistic conjugates.[37]

4.6 Concluding Remarks

Successful isolation and structure elucidation of the active compounds within the hexane extracts of the roots of *Pentalinon andrieuxii* (Kinghorn group) provided a promising antileishmanial lead compound, pentalinonsterol. Optimization of the previously reported synthetic route (Fuchs Group) towards pentalinonsterol has facilitated extensive biological studies (Satoskar, Parinandi, and Ainslie Groups) providing convincing evidence of pentalinonsterol's antileishmanial properties. Of importance was the identification of a dual mechanism of action in the eradication of leishmaniasis parasites through a combination of destructive membrane alterations and an induced host immune response. Initial analogue development focused on probing the importance of the pre-determined pharmacophore, the A-ring α,β-unsaturated ketone and the C17 side chain, via structure-activity relationship studies. Non-comprehensive biological data gave evidence supporting the importance of these moieties.

Current analogue development is focused on improving the pharmacological properties of pentalinonsterol itself through the introduction of a hydroxyl handle for the attachment of water solubilizing groups as well as mechanistic probes. We have obtained key methyl ketone intermediates from both deoxycholic acid and chenodeoxycholic acid and have successfully performed the alkylation on silyl protected material. We are optimistic about the success of the Wittig olefination once we acquire more material to investigate reaction conditions. A-ring functionalization will then provide the hydroxyl containing analogues, a sequence for which we have literature precedence; selective C3 alcohol deprotection, oxidation to the ketone, and IBX oxidation to install the α,β-unsaturated ketone. With these analogues in hand we hope to learn more about pentalinonsterol's mechanism of action and improve its oral bioavailability.

Chapter 5: Experimentals

Note about Sterol Characterization: Not all protons present in the molecules synthesized are listed in the ^{1}H NMR characterization data due to the difficulty in interpreting the aliphatic region (between 0.5 and 2.5 ppm) of this class of compounds. Chemical shifts are reported for proton NMR peaks considered to be of diagnostic value in accordance with examples in the chemical literature. Specifically, this includes any peaks occurring downfield of 2.5 ppm as well as methyl groups observed from 0-2.5 ppm.

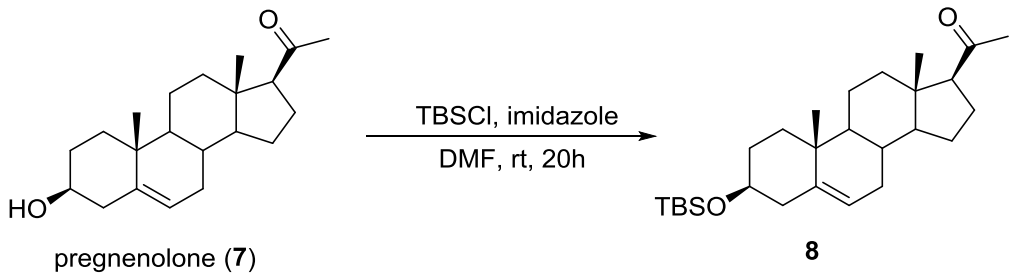

pregnenolone (**7**) **8**

Silyl ether 8. A solution of pregnenolone (3.000 g, 9.749 mmol), *tert*-butyldimethylsilyl chloride (2.143 g, 14.21 mmol), and imidazole (0.807 g, 11.85 mmol) in DMF (158 mL) was stirred at 21 °C overnight. The reaction mixture was quenched with cold deionized water. The resulting white precipitate was collected via vacuum filtration and washed with cold deionized water (3 x 10 mL) to obtain the silyl ether **8** (3.896 g, 9.045 mmol, 95%) as a white powder: mp 163 °C; ^{1}H NMR (400 MHz, $CDCl_3$) δ 5.31 (m, 1H), 3.48 (m, 1H), 2.53 (t, J = 8.9 Hz, 1H), 2.12 (s, 3H), 1.81 (dt, J = 13.2, 3.4 Hz, 1H), 0.98 (s, 3H), 0.88 (s, 9H), 0.62 (s, 3H), 0.05 (s, 6H); ^{13}C NMR (100 MHz, $CDCl_3$) δ 209.74, 141.69, 121.01, 72.68, 63.87, 57.10, 50.20, 44.16, 42.90, 39.01, 37.52, 36.74, 32.18, 32.00, 31.95, 31.71, 26.08, 24.63, 22.94, 21.21, 19.56, 18.41, 13.36, -4.44; IR (film): 1701 cm−1; HRMS-TOF m/z (M + Na)+ calcd for $C_{27}H_{46}O_2Si$ 453.3165, found 453.3165.

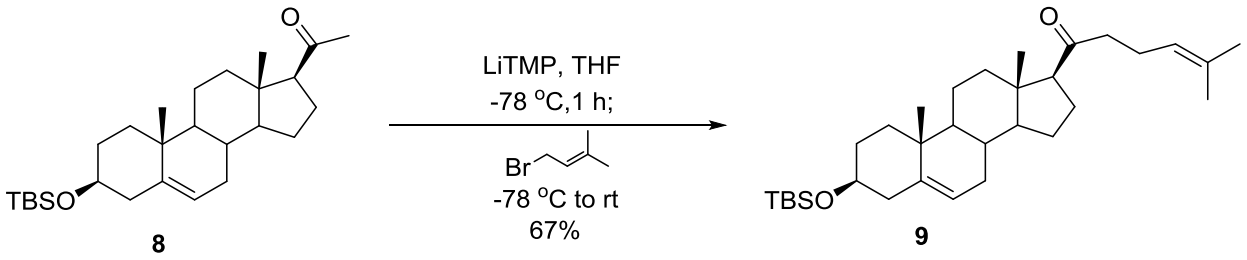

Mono-alkylated silyl ether 9. To a solution of tetramethylpiperidine (0.296 mL, 1.741 mmol) in THF (5.7 mL) at -78 °C was added *n*-butyl lithium (2.5 M in hexanes, 0.650 mL, 1.625 mmol). The resulting solution was allowed to stir for 35 minutes at -78 °C before the addition of a solution of **8** (0.500 g, 1.161 mmol) in THF (5.7 mL). After 3 h of stirring at -78 °C, dimethyl allyl bromide (0.268 mL, 2.321 mmol) was added dropwise to the reaction mixture, warmed to 21 °C, and stirred overnight. The reaction was quenched with excess aqueous ammonium chloride. The organic layer was removed and the aqueous layer was extracted three times with ethyl acetate. The combined organic layers were then dried with anhydrous sodium sulfate and concentrated under reduced pressure. The crude product was purified by silica gel column chromatography (EtOAc:DCM:hexanes, 1:1:98) to afford pure mono-alkylated product **9** (0.397 g, 0.796 mmol, 68%) as a white solid: mp 120-121 °C; ^{1}H NMR (300 MHz, $CDCl_3$) δ 5.31 (d, *J* = 5.2 Hz, 1H), 5.08 (t, 1H), 3.48 (m, 1H), 2.51 (t, *J* = 8.9 Hz, 1H), 1.66 (s, 3H), 1.60 (s, 3H), 1.00 (s, 3H), 0.88 (s, 9H), 0.61 (s, 3H), 0.06 (s, 6H); ^{13}C NMR (101 MHz, $CDCl_3$) δ 211.32, 141.65, 132.51, 123.33, 121.00, 72.66, 63.07, 57.14, 50.22, 44.44, 44.32, 42.90, 39.11, 37.52, 36.73, 32.18, 32.00, 31.96, 26.06, 25.81, 24.67, 23.06, 22.56, 21.21, 19.55, 18.37, 17.78, 13.48, -4.46; IR (film): 1704 cm−1; HRMS-TOF m/z (M + Na)+ calcd for $C_{32}H_{54}O_2Si$ 521.3791, found 521.3814.

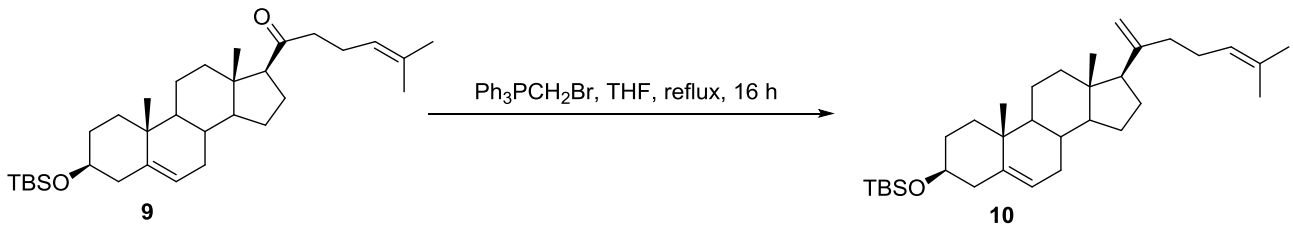

Methylene 10. To a solution of methyltriphenylphosphonium bromide (3.940 g, 11.02 mmol) in THF (5.5 mL) at 0 °C was added *n*-butyl lithium (2.5 M in hexanes, 4.19 mL, 10.47 mmol). The resulting reaction mixture was stirred at 0 °C for 1 hour before adding a solution of **9** (0.550 g, 1.102 mmol) in THF (5.5 mL). The reaction was brought to reflux and stirred overnight before being quenched with deionized water. The organic layer was removed and the aqueous layer was extracted three times with ethyl acetate. Combined organic layers were dried over anhydrous sodium sulfate and concentrated under reduced pressure. The crude mixture was then purified via silica gel column chromatography (EtOAc-hexanes, 2:98) to obtain pure **10** (0.489 g, 0.984 mmol, 89%) as a white solid: mp 86 °C; ^{1}H NMR (400 MHz, $CDCl_3$) δ 5.32 (d, *J* = 5.2 Hz, 1H), 5.11 (m, 1H), 4.88 (s, 1H), 4.79 (s, 1H), 3.48 (m, 1H), 2.27 (t, *J* = 12.0 Hz, 1H), 1.68 (s, 3H), 1.61 (s, 3H), 0.99 (s, 3H), 0.87 (s, 9H), 0.57 (s, 3H), 0.06 (s, 6H); ^{13}C NMR (101 MHz, $CDCl_3$) δ 149.49, 141.76, 131.58, 124.53, 121.23, 109.54, 72.76, 72.00, 56.84, 56.15, 50.50, 43.24, 42.96, 38.88, 37.84, 37.54, 36.79, 32.45, 32.22, 32.01, 27.30, 26.09, 25.99, 25.87, 24.38, 21.27, 19.61, 18.43, 17.88, 12.90, -4.44; IR (film): 2928 cm−1.

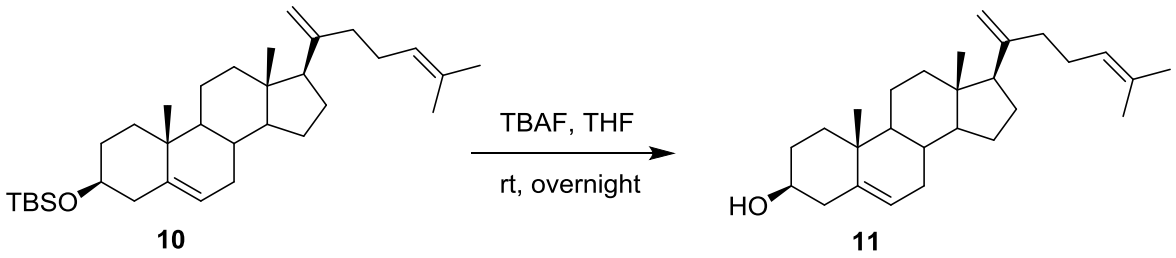

β,γ-alcohol 11. A solution of **10** (0.124 g, 0.250 mmol) and tetrabutylammonium fluoride (1.0 M in THF, 0.5 mL, 0.5 mmol) in THF (1.25 mL) was stirred at 21 °C overnight. The reaction mixture was concentrated under reduced pressure and the resulting residue was purified by silica gel column chromatography (EtOAc-DCM-hexanes, 1:4:5) to give the corresponding β,γ-alcohol **11** (0.094 g, 0.246 mmol, 94%) as a white solid: mp 89-91 °C; ^{1}H NMR (400 MHz, $CDCl_3$) δ 5.36 (d, *J* = 5.1 Hz, 1H), 5.11 (m, 1H), 4.88 (s, 1H), 4.79 (s, 1H), 3.53 (m, 1H), 1.69 (s, 3H), 1.58 (s, 3H), 0.99 (s, 3H), 0.58 (s, 3H); ^{13}C NMR (101 MHz, $CDCl_3$) δ 149.45, 140.93, 131.59, 124.52, 121.78, 109.56, 72.00, 71.92, 56.79, 56.14, 50.40, 43.22, 42.43, 38.85, 37.84, 37.40, 36.69, 32.43, 31.96, 31.79, 27.30, 25.98, 25.87, 24.37, 21.28, 19.57, 17.87, 12.91; HRMS-TOF m/z (M + Na)+ calcd for $C_{27}H_{42}O$ 405.3133, found 405.3151.

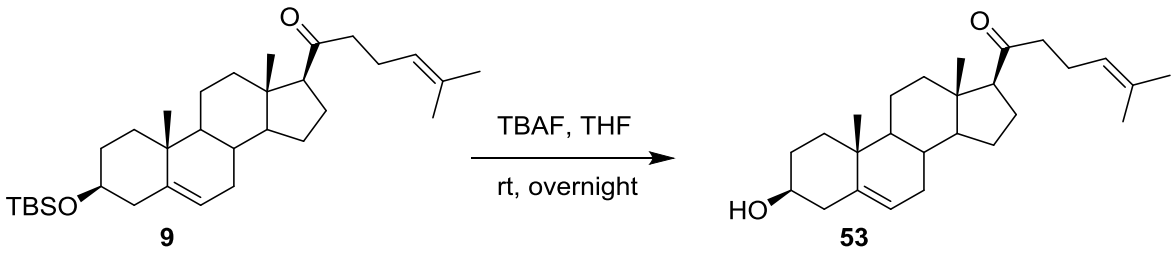

β,γ-alcohol 53. A solution of **9** (0.090 g, 0.180 mmol) and tetrabutylammonium fluoride (1.0 M in THF, 0.271 mL, 0.271 mmol) in THF (0.902 mL) was stirred at 21 °C overnight. The reaction mixture was concentrated under reduced pressure and the resulting residue was purified by silica gel column chromatography (acetone-hexanes, 5:95) to give the corresponding β,γ-alcohol **53** (0.059 g, 0.153 mmol, 85%) as a white solid: ^{1}H NMR (250 MHz, $CDCl_3$) δ 5.34 (d, 1H), 5.06 (m, 1H), 3.52 (m, 1H), 1.67 (s, 3H), 1.61 (s, 3H), 1.00 (s, 3H), 0.61 (s, 3H).

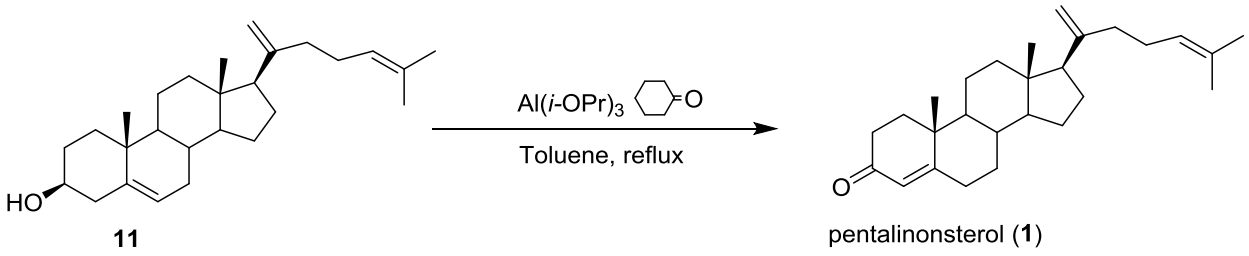

Pentalinonsterol (1). To a solution of **11** (0.434 g, 1.135 mmol) and cyclohexanone (1.175 mL, 11.35 mmol) in toluene (22.7 mL) at reflux was added aluminum isopropoxide (0.116 g, 0.568 mmol). The reaction was stirred at reflux overnight. The reaction mixture was concentrated under reduced pressure, taken up in deionized water, and extracted three times with ethyl acetate. The crude mixture was purified by silica gel column chromatography (EtOAc:hexanes, gradient 7-10% EtOAc, 1% EtOAc every 100 mL) to afford pure pentalinonsterol (**1**) (0.386 g, 1.014 mmol, 89%) as a white solid: mp 89-91 °C; ^{1}H NMR (400 MHz, $CDCl_3$) δ 5.73 (s, 1H), 5.10 (m, 1H), 4.89 (s, 1H), 4.79 (s, 1H), 1.68 (s,3H), 1.60 (s, 3H), 1.16 (s, 3H), 0.61 (s, 3H); ^{13}C NMR (101 MHz, $CDCl_3$) δ 199.83, 171.75, 149.18, 131.66, 124.42, 123.93, 109.82, 72.00, 56.05, 55.90, 54.08, 43.25, 38.79, 38.67, 37.78, 36.16, 35.84, 34.12, 33.06, 32.09, 27.28, 25.92, 25.86, 24.25, 21.23, 17.87, 17.54, 13.00; HRMS-TOF m/z (M + Na)+ calcd for C27H42O 405.3133, found 405.3151.

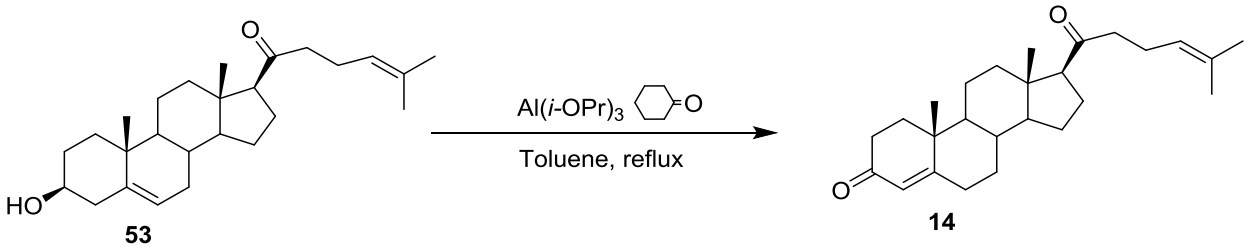

α,β-unsaturated ketone 14. To a solution of **53** (0.057 g, 0.147 mmol) and cyclohexanone (0.153 mL, 1.474 mmol) in toluene (2.95 mL) at reflux was added aluminum isopropoxide (0.015 g, 0.074 mmol). The reaction was stirred at reflux overnight. The reaction mixture was concentrated under reduced pressure, taken up in deionized water, and extracted three times with ethyl acetate. The crude mixture was purified by silica gel column chromatography (acetone-hexanes, 5:95) to afford pure **14** (0.049 g, 0.128 mmol, 87%) as a clear oil: ^{1}H NMR (300 MHz, $CDCl_3$) δ 5.71 (s, 1H), 5.04 (t, *J* = 6.8 Hz, 1H), 1.67 (s, 3H), 1.59 (s, 3H), 1.15 (s, 3H), 0.63 (s, 3H).

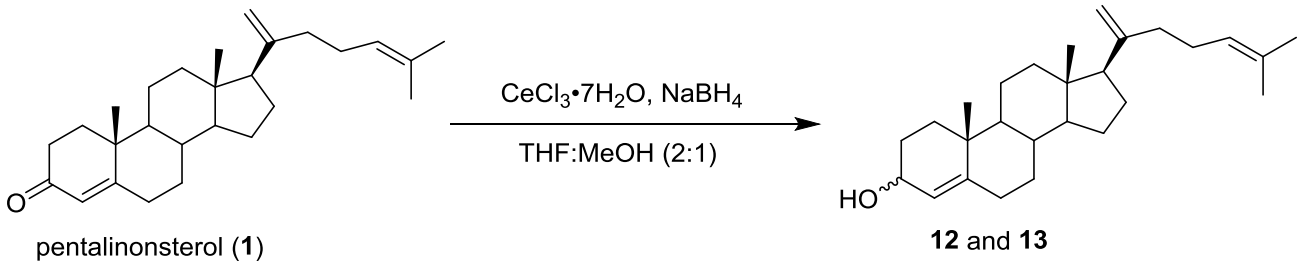

pentalinonsterol (**1**) **12** and **13**

Allyl alcohols 12 and 13. A solution of pentalinonsterol (**1**) (0.030, 0.079 mmol) and cerium (III) chloride heptahydrate (0.029 g, 0.079 mmol) in THF-MeOH (2:1, 0.790 mL) was cooled to 0 °C before the portion wise addition of sodium borohydride (0.019 g, 0.502 mmol). The reaction mixture was allowed to warm to 21 °C and stirred overnight. The reaction was quenched with 2M HCl. The organic layer was removed and the aqueous layer was extracted three times with ethyl acetate. Combined organic layers were washed with brine, dried over anhydrous sodium sulfate, and concentrated under reduced pressure. The crude mixture was then purified via silica gel column chromatography (EtOAc:hexanes, gradient 5-10% EtOAc, 1% EtOAc every 100 mL) to afford two diastereomers (d.r. 3.4:1, 56% overall yield):

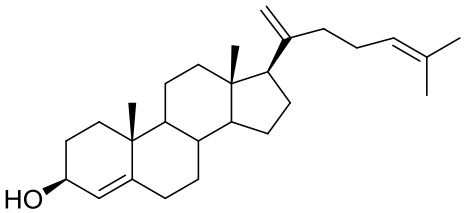

12

(0.013 g, 0.034 mmol, 43%) as a white solid: ^{1}H NMR (400 MHz, $CDCl_3$) δ 5.28 (s, 1H), 5.11 (s, 1H), 4.88 (s, 1H), 4.78 (s, 1H), 4.14 (s, 1H), 1.68 (s, 3H), 1.61 (s, 3H), 1.07 (s, 3H), 0.58 (s, 3H); ^{13}C NMR (101 MHz, $CDCl_3$) δ 149.46, 147.86, 131.57, 124.53, 123.51, 109.62, 68.13, 56.24, 56.20, 54.77, 43.37, 38.94, 37.81, 37.55, 36.53, 35.54, 33.20, 32.36, 29.69, 27.32, 25.98, 25.85, 24.31, 21.26, 19.11, 17.86, 13.03; IR (film): 3330, 2930, 2849 cm^{-1}.

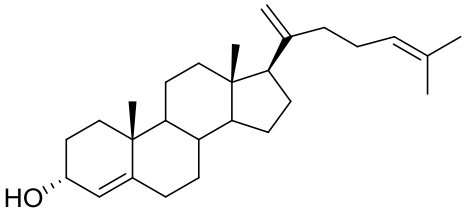

13

(0.004 g, 0.010 mmol, 13%) as a white solid: ^{1}H NMR (250 MHz, $CDCl_3$) δ 5.47 (d, *J* = 4.7 Hz, 1H), 5.12 (s, 1H), 4.88 (s, 1H), 4.79 (s, 1H), 4.07 (s, 1H), 1.69 (s, 5H), 1.61 (s, 4H), 0.98 (s, 3H), 0.59 (s, 3H).

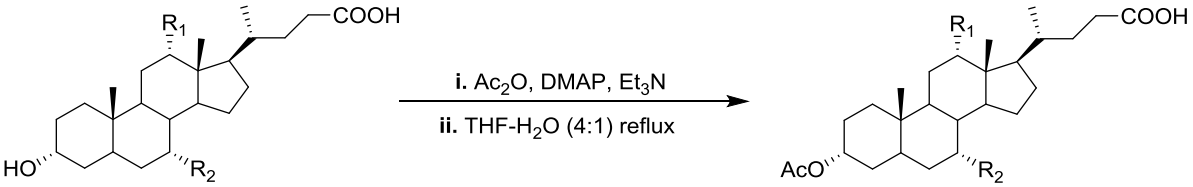

18 R1=OH; **R2**=H
deoxycholic acid
19 R1=H; **R2**=OH
chenodeoxycholic acid

26 R1=OAc; **R2**=H
27 R1=H; **R2**=OAc

General procedure for acylation:

To a solution of a cholic acid derivative in acetic anhydride (23 equiv.) at 0 °C was added dimethylaminopyridine (0.06 equiv.) and triethylamine (16 equiv.). The resulting reaction mixture was stirred at 21 °C overnight. The reaction was quenched with deionized water at 0 °C. The organic layer was removed and the aqueous layer was extracted three times with ethyl acetate. Combined organic layers were washed with 1 M HCl and deionized water before being dried over anhydrous sodium sulfate and concentrated under reduced pressure. The crude product was then dissolved in a THF-H_2O, 4:1 solution and refluxed overnight. The organic layer was removed and the aqueous layer was extracted three times with ethyl acetate. Combined organic layers were concentrated under reduced pressure. The crude mixture was purified via silica gel column chromatography (EtOAc-hexanes, 33:67) to obtain the corresponding products.

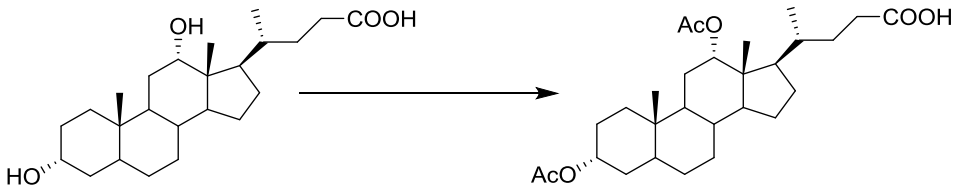

18 **26**

Acylated deoxycholic acid 26. Using deoxycholic acid (**18**) (1.500 g, 3.82 mmol) as the starting material, the above general procedure afforded compound **26** (1.928 g, 3.606 mmol, 94%), obtained as a white solid: ^{1}H NMR (400 MHz, $CDCl_3$) δ 5.08 (s, 1H), 4.70 (m, 1H), 2.10 (s, 3H), 2.03 (s, 3H), 0.89 (s, 3H), 0.81 (d, J = 6.3 Hz, 3H), 0.73 (s, 3H); ^{13}C NMR (101 MHz, $CDCl_3$) δ 179.85, 170.77, 170.65, 76.06, 74.37, 49.59, 47.73, 45.18, 41.97, 35.83, 34.87, 34.80, 34.55, 34.19, 32.41, 31.03, 30.75, 27.47, 27.03, 26.78, 26.01, 25.79, 23.57, 23.21, 21.60, 21.51, 17.64, 12.56; IR (film): 2946, 2870, 1735 cm^{-1}.

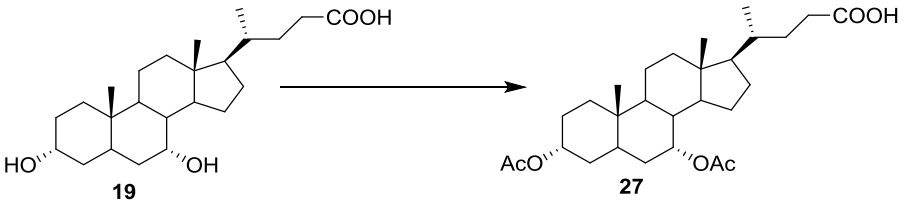

Acylated chenodeoxycholic acid 27. Using chenodeoxycholic acid (**19**) (3.000 g, 7.642 mmol) as the starting material, the above general procedure afforded **27** (2.794 g, 5.862 mmol, 77%) as a white solid: ^{1}H NMR (400 MHz, $CDCl_3$) δ 4.87 (s, 1H), 4.58 (m, 1H), 2.04 (s, 3H), 2.02 (s, 3H), 0.928 (d, J = 6.3 Hz, 3H), 0.925 (s, 3H), 0.65 (s, 3H); ^{13}C NMR (101 MHz, $CDCl_3$) δ 179.92, 170.83, 170.62, 74.34, 71.40, 55.88, 50.54, 42.85, 41.09, 39.64, 38.04, 35.36, 35.04, 34.93, 34.77, 34.21, 31.46, 31.00, 30.84, 28.14, 26.93, 23.68, 22.82, 21.72, 21.61, 20.79, 18.39, 11.85; IR (film): 2941, 2871, 1733 cm^{-1}.

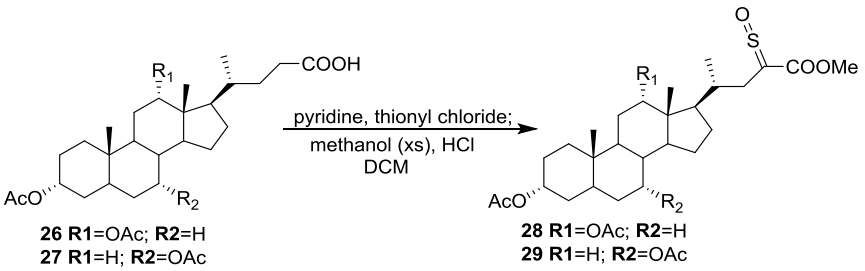

26 R1=OAc; **R2**=H
27 R1=H; **R2**=OAc

28 R1=OAc; **R2**=H
29 R1=H; **R2**=OAc

General procedure for sulphine formation:

To a solution of an acylated cholic derivative and pyridine (10 equiv.) in DCM (0.2 M) at 10 °C was added thionyl chloride (2.2 equiv.). The reaction was allowed to stir 30 minutes at 21 °C before being cooled to 0 °C for the addition of excess methanol (1 M). The reaction mixture was stirred for 10 minutes at 0 °C before being quenched with 0.5 M HCl (0.05 M). The organic layer was removed and the aqueous layer was extracted three times with DCM. Combined organic layers were dried with anhydrous sodium sulfate and concentrated under reduced pressure. The crude mixture was purified via silica gel column chromatography (EtOAc-hexanes, 13:87) to afford the corresponding products.

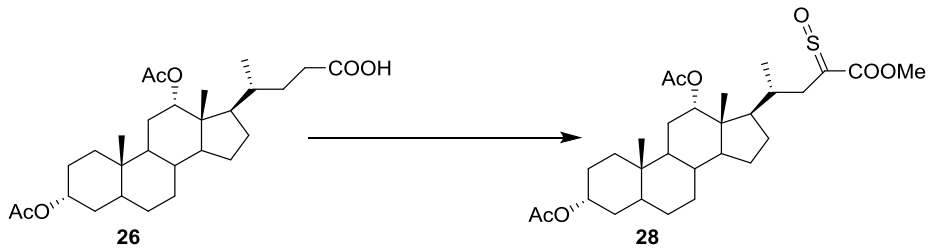

Sulphine 28. Using acylated deoxycholic acid **26** (0.500 g, 1.048 mmol) as the starting material, the above general procedure afforded sulphine **28** (0.286 g, 0.533 mmol, 51%) as a white powder: ^{1}H NMR (400 MHz, $CDCl_3$) δ 5.04 (s, 1H), 4.68 (m, 1H), 3.84 (s, 3H), 2.87 (dd, *J* = 12.5, 10.2 Hz, 1H), 2.70 (d, *J* = 12.4 Hz, 1H), 2.09 (s, 3H), 2.02 (s, 3H), 0.89 (s, 3H), 0.77 (d, *J* = 5.6 Hz, 3H), 0.72 (s, 3H); ^{13}C NMR (101 MHz, $CDCl_3$) δ 186.67, 170.68, 170.55, 164.22, 75.76, 74.27, 52.79, 49.61, 48.71, 45.42, 41.91, 36.07, 35.79, 34.82, 34.45, 34.36, 34.13, 32.36, 27.53, 26.97, 26.74, 25.94, 25.71, 23.58, 23.18, 21.59, 21.57, 18.04, 12.58.

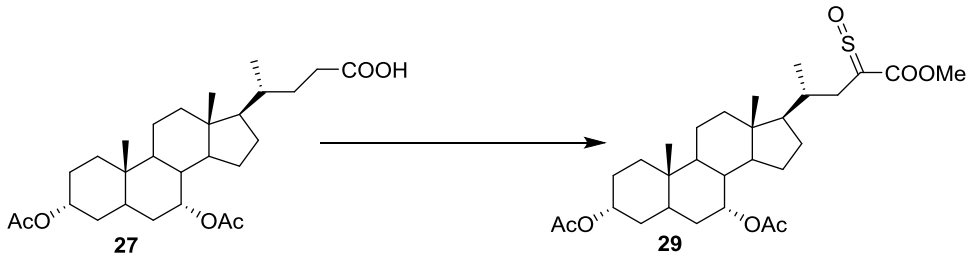

Sulphine 29. Using acylated chenodeoxycholic acid **27** (0.330 g, 0.692 mmol) as the starting material, the above general procedure afforded sulphine **29** (0.167 g, 0.311mmol, 45%) as a white powder: ^{1}H NMR (400 MHz, $CDCl_3$) δ 4.89 (s, 1H), 4.59 (m, 1H), 3.85 (s, 3H), 2.91 (dd, *J* = 12.6, 10.8 Hz, 1H), 2.71 (dd, *J* = 12.8, 3.2 Hz, 1H), 2.06 (s, 3H), 2.03 (s, 3H), 0.93 (s, 3H), 0.91 (d, *J* = 6.6 Hz, 3H), 0.66 (s, 3H); ^{13}C NMR (101 MHz, $CDCl_3$) δ 186.91, 170.78, 170.56, 164.30, 74.29, 71.33, 57.01, 52.79, 50.61, 43.18, 41.10, 39.51, 38.06, 36.90, 35.05, 34.95, 34.79, 34.64, 34.18, 31.47, 28.34, 26.94, 23.77, 22.83, 21.75, 21.63, 20.76, 18.68, 11.86; IR (film): 2941, 2870, 1731 cm^{-1}.

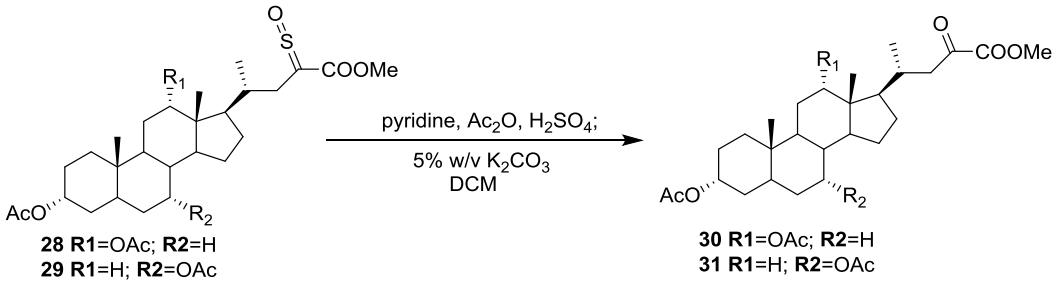

28 R1=OAc; **R2**=H
29 R1=H; **R2**=OAc

30 R1=OAc; **R2**=H
31 R1=H; **R2**=OAc

General procedure for α-ketoester formation:

To a sulphine was added a prepared solution (0.56 M) of acetic anhydride (1.15 mL) and sulfuric acid (35 µL, 95%) in DCM (8.8 mL). The resulting reaction mixture was stirred at 21 °C for 15 minutes before dilution with DCM (0.05 M) and potassium carbonate (0.11 M, 5% w/v). The reaction was stirred overnight and then quenched with deionized water. The organic layer was removed and the aqueous layer was extracted three times with DCM. Combined organic layers were washed with brine, dried over anhydrous sodium sulfate, and concentrated under reduced pressure. The crude mixture was purified via silica gel column chromatography (EtOAc-hexanes, 15:85) to afford the corresponding products.

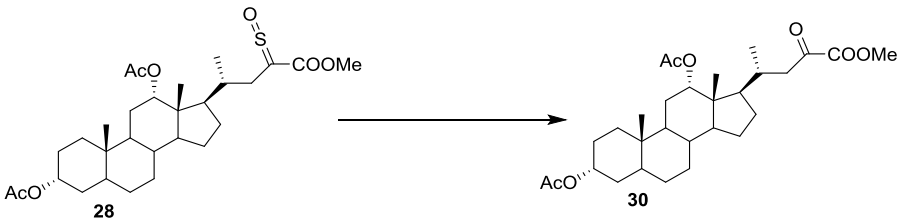

α-ketoester 30. Using sulphine **28** (0.500 g, 0.932 mmol) as the starting material, the above general procedure afforded α-ketoester **30** (0.396 g, 0.785 mmol, 84%) as a white solid: ^{1}H NMR (400 MHz, $CDCl_3$) δ 5.05 (s, 1H), 4.68 (m, 1H), 3.84 (m, 3H), 2.85 (dd, *J* = 17.1, 3.1 Hz, 1H), 2.59 (dd, *J* = 17.1, 9.3 Hz, 1H), 2.10 (s, 3H), 2.01 (s, 3H), 0.89 (s, 3H), 0.84 (d, *J* = 6.5 Hz, 3H), 0.75 (s, 3H); ^{13}C NMR (101 MHz, $CDCl_3$) δ 194.26, 170.65, 170.50, 161.89, 75.80, 74.28,

53.03, 49.63, 47.62, 46.03, 45.25, 41.93, 35.79, 34.84, 34.50, 34.16, 32.39, 31.83, 27.77, 26.98, 26.75, 25.96, 25.74, 23.53, 23.18, 21.56, 21.48, 18.98, 12.50.

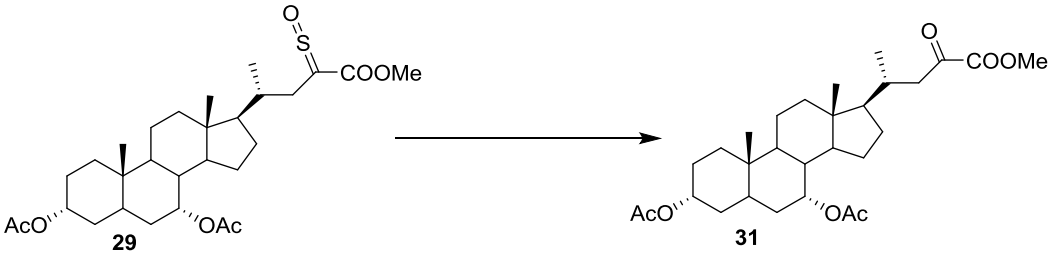

α-ketoester 31. Using sulphine **29** (0.500g, 0.932 mmol) as the starting material, the above general procedure afforded α-ketoester **31** (0.311 g, 0.616 mmol, 66%) as a white solid: ^{1}H NMR (400 MHz, $CDCl_3$) δ 4.88 (d, *J* = 2.4 Hz, 1H), 4.58 (m, 1H), 3.86 (s, 3H), 2.89 (dd, *J* = 16.8, 3.0 Hz, 1H), 2.58 (dd, *J* = 16.9, 9.7 Hz, 1H), 2.05 (s, 3H), 2.03 (s, 3H), 0.96 (d, *J* = 6.5 Hz, 3H), 0.93 (s, 3H), 0.69 (s, 3H); ^{13}C NMR (101 MHz, $CDCl_3$) δ 194.51, 170.76, 170.53, 161.94, 74.29, 71.31, 56.04, 53.05, 50.60, 46.28, 42.99, 41.09, 39.53, 38.05, 35.04, 34.95, 34.79, 34.20, 32.41, 31.47, 28.41, 26.94, 23.69, 22.82, 21.72, 21.63, 20.76, 19.81, 11.87; IR (film): 2940, 2871, 1732 cm^{-1}.

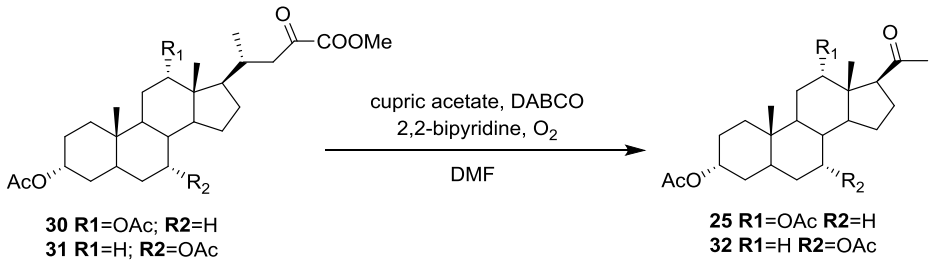

30 R1=OAc; **R2**=H
31 R1=H; **R2**=OAc

25 R1=OAc **R2**=H
32 R1=H **R2**=OAc

General procedure for methyl ketone formation:

A solution of an α-ketoester, 1,4-diazabicyclo[2.2.2]octane (0.044 g, 0.392 mmol), cupric acetate (0.031 g, 0.157 mmol), and 2,2'-dipyridyl (0.029 g, 0.188 mmol) in DMF (26.1 mL) was stirred at 50 °C open to the atmosphere for 6.5 days. The reaction mixture was then cooled to 0 °C and quenched with deionized water. The organic layer was removed and the aqueous layer was

extracted three times with DCM. Combined organic layers were washed with brine, dried over anhydrous sodium sulfate, and concentrated under reduced pressure. The crude mixture was purified via silica gel column chromatography (EtOAc-hexanes, 15:85) to afford the corresponding products.

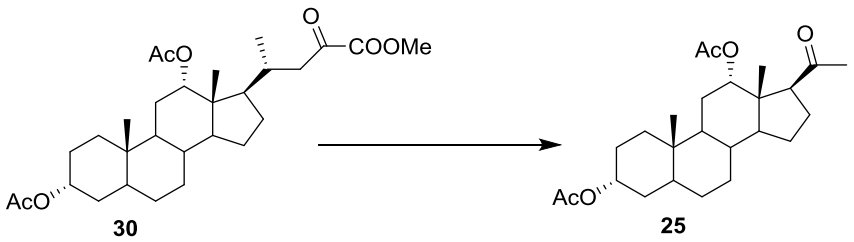

Methyl ketone 25. Using α-ketoester **30** (0.396 g, 0.785 mmol) as the starting material, the above general procedure afforded methyl ketone **25** (0.297 g, 0.710 mmol, 90%) as a white solid: ^{1}H NMR (300 MHz, $CDCl_3$) δ 5.11 (s, 1H), 4.67 (m, 1H), 2.93 (t, *J* = 8.9 Hz, 1H), 2.14 (s, 3H), 2.01 (s, 3H), 1.99 (s, 3H), 0.88 (s, 3H), 0.65 (s, 3H); ^{13}C NMR (101 MHz, $CDCl_3$) δ 208.90, 170.67, 170.54, 74.62, 74.23, 55.76, 49.78, 46.87, 41.91, 35.77, 34.90, 34.62, 34.25, 32.41, 31.24, 26.95, 26.78, 26.05, 25.78, 23.82, 23.17, 22.44, 21.60, 21.55, 14.00.

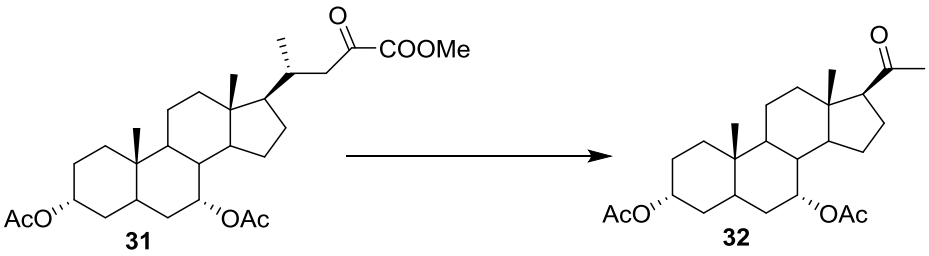

Methyl ketone 32. Using α-ketoester **31** (0.174 g, 0.345 mmol) as the starting material, the above general procedure afforded methyl ketone **32** (0.135 g, 0.323 mmol, 93%) as a white solid: ^{1}H NMR (400 MHz, $CDCl_3$) δ 4.86 (s, 1H), 4.56 (m, 1H), 2.50 (t, *J* = 9.3 Hz, 1H), 2.08 (s, 3H), 2.02 (s, 3H), 2.00 (s, 3H), 0.90 (s, 3H), 0.57 (s, 3H).

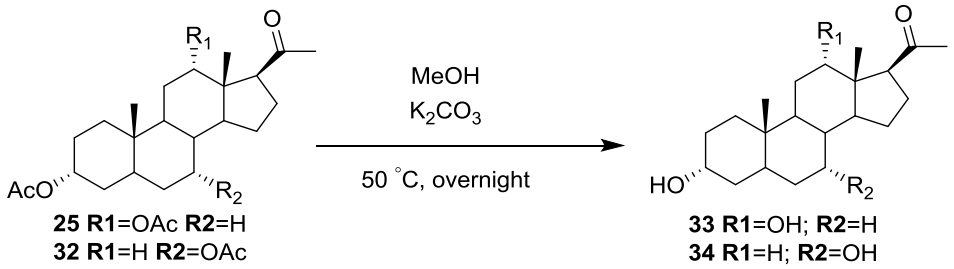

25 R1=OAc **R2**=H
32 R1=H **R2**=OAc

33 R1=OH; **R2**=H
34 R1=H; **R2**=OH

General procedure for acetate deprotection:

A solution of a methyl ketone and potassium carbonate (5 equiv.) in methanol (0.05 M) was stirred at 50 °C for 24 h. The reaction mixture was concentrated under reduced pressure, taken up in deionized water, and extracted with EtOAc three times. The combined organic layers were washed with brine, dried over anhydrous sodium sulphate, and concentrated under reduced pressure to yield the corresponding products.

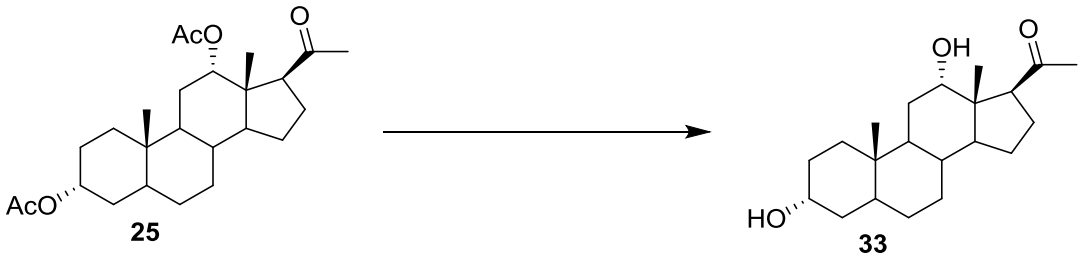

25 **33**

Deoxycholic methyl ketone 33. Using methyl ketone **25** (0.109 g, 0.261 mmol) as the starting material, the above general procedure afforded crude deoxycholic methyl ketone **33** (0.074 g) as a white solid. The crude product was checked by proton NMR and then carried forward into the next reaction without further purification: ^{1}H NMR (300 MHz, $CDCl_3$) δ 3.98 (t, *J* = 2.8 Hz, 1H), 3.63 (m, 1H), 3.12 (t, *J* = 9.3 Hz, 1H), 2.14 (s, 3H), 0.91 (s, 3H), 0.63 (s, 3H).

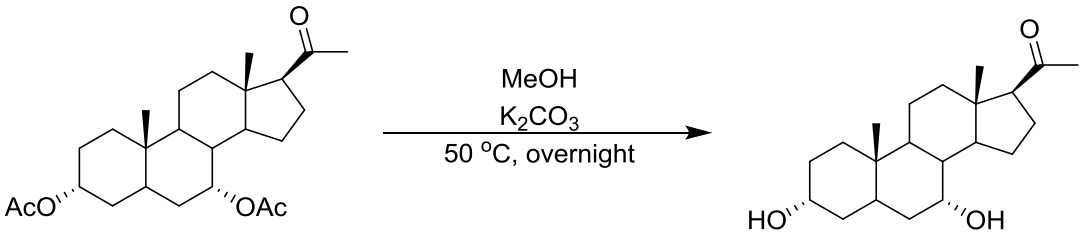

Chenodeoxycholic methyl ketone 34. Using methyl ketone **32** (0.110 g, 0.263 mmol) as the starting material, the above general procedure afforded crude chenodeoxycholic methyl ketone **34** (0.078 g) as a white solid. Existence of desired product was confirmed by proton NMR.

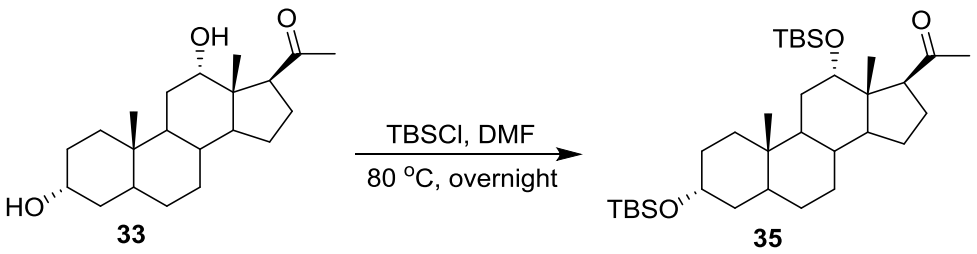

Di-silyl ether 35. A solution of crude deoxycholic methyl ketone **33** (0.073 g), tert-butyldimethylsilyl chloride (9.5 equiv.), and imidazole (10 equiv.) in DMF (0.05 M) was stirred at 80 °C overnight. The reaction mixture was quenched with deionized water. The organic layer was removed and the aqueous layer was extracted three times with DCM. Combined organic layers were washed with brine, dried over anhydrous sodium sulfate, and concentrated under reduced pressure. The crude mixture was purified via silica gel column chromatography (EtOAc-hexanes, 2:98) to afford pure di-silyl ether **35** (0.078 g, 0.139 mmol, 53% over 2 steps) as a white solid: (^{1}H NMR (400 MHz, $CDCl_3$) δ 4.10 (s, 1H), 3.54 (m, 1H), 2.93 (t, J = 9.9 Hz, 1H), 2.05 (s, 3H), 0.92 (s, 9H), 0.87 (s, 3H), 0.87 (s, 9H), 0.70 (s, 3H), 0.06 (s, 3H), 0.02 (s, 6H), -0.01 (s, 3H); ^{13}C NMR (101 MHz, $CDCl_3$) δ 210.47, 72.51, 72.38, 55.65, 47.86, 47.56, 42.41, 37.27, 35.92, 35.54, 34.41, 33.81, 31.39, 30.58, 28.38, 27.52, 26.36, 26.29, 26.01, 24.15, 23.94, 23.56, 18.37, 18.19, 13.94, -3.58, -4.36, -4.74; IR (film): 2952, 2927, 2857, 1703 cm^{-1}.

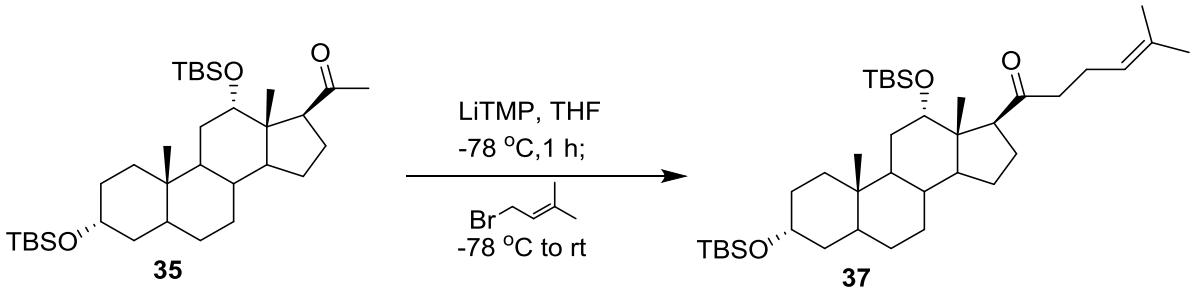

Mono-alkylated di-silyl ether 37. To a solution of tetramethylpiperidine (0.034 mL, 0.202 mmol) in THF (0.63 mL) at -78 °C was added *n*-butyl lithium (2.5 M in hexanes, 0.076 mL, 0.189 mmol). The resulting solution was allowed to stir for 35 minutes at -78 °C before the addition of a solution of di-silyl ether **35** (0.071 g, 0.126 mmol) in THF (0.63 mL). After 1 h of stirring at -78 °C, dimethyl allyl bromide (0.029 mL, 0.252 mmol) was added drop wise to the reaction mixture, warmed to 21 °C, and stirred overnight. The reaction was quenched with excess aqueous ammonium chloride. The separated and aqueous layer was extracted with ethyl acetate. The combined organic layers were then dried with anhydrous sodium sulfate and concentrated under reduced pressure. The presence of mono-alkylated di-silyl ether **37** in the crude material was confirmed by proton NMR, but the purity of the compound is not sufficient for complete compound characterization.

References

[1] [a]Centers for Disease Control and Prevention. Parasite – Leishmaniasis. http://www.cdc.gov/parasites/leishmaniasis/ (accessed March 23, 2015).

[b]World Health Organization. Leishmaniasis. http://www.who.int/leishmaniasis/en/ (accessed March 24, 2015).

[2] Medscape. Drugs and Disease: Leishmaniasis. http://emedicine.medscape.com/article/220298-overview#showall (accessed March 25, 2015).

[3] Neuber, H. Leishmaniasis. *Journal of the German Society of Dermatology* **2008**, *6(9)*, 754.

[4] Abdelhamid, D. A. S. Natural Products as Lead Compounds for Drug Development. PhD. Dissertation, The Ohio State University, Columbus, OH, **2011**.

[5] Alvar, J.; Ve´lez, I. D.; Bern, C.; Herrero, M.; Desjeux, P. et al. Leishmaniasis Worldwide and Global Estimates of Its Incidence. *PLoS ONE* **2012**, *7(5)*: e35671. doi:10.1371/journal.pone.0035671

[6] Nail, A. M.; Imam, A. M. Visceral leishmaniasis: Clinical and demographic features in an African population. *Pak J Med Sci* **2013**, *29(2)*, 485-489.

[7] Choi, C. M.; Lerner, E. A. Leishmaniasis as an Emerging Infection. *Journal of Investigative Dermatology Symposium Proceedings* **2001**, *6*, 175-182.

[8] Pape, P. L. Development of new antileishmanial drugs – current knowledge and future prospects. *Journal of Enzyme Inhibition and Medicinal Chemistry* **2008**, *23(5)*, 708–718.

[9] Hussain, H.; Al-Harrasi, A.; Al-Rawahi, A.; Green, I. R.; Gibbons, S. Fruitful Decade for Antileishmanial Compounds from 2002 to Late 2011. *Chemical Reviews* **2014**, *114(20)*, 10369-10428.

[10] Pulido Salas, M. T.; Serralta Peraza, L. Lista Anotada de las Plantas Medicinales de Uso Actual en el Estado de Quintana Roo, México. *Centro de Investigaciones*

de Quintana Roo, Chetumal, Quintana Roo, México. **1993**

[11] Argüeta, A.; Cano, L.; Rodarte, M. Atlas de las Plantas de la Medicina Tradicional Mexicana, vol. 2. *Instituto Nacional Indigenista, Mexico, DF*. **1994**

[12] Pan, L.; Lezama-Davila, C. M.; Isaac-Marquez, A. P.; Calomeni, E. P.; Fuchs, J. R.; Satoskar, A. R.; Kinghorn, A. D. Sterols with antileishmanial activity isolated from the roots of *Pentalinon andrieuxii*. *Phytochemistry* **2012**, *82*, 128-135.

[13] Uskokovic, M.; Dorfman, R. I.; Gut, M. *J. Org. Chem.* **1958**, *23(12)*, 1947-1951.

[14] Reich, R.; Keana, J. F. W. *Synthetic Communications* **1972**, *2(5)*, 323.

[15] Gupta, G.; Peine, K. J.; Abdelhamid, D.; Snider, H.; Shelton, A. B.; Rao, L.; Kotha, S. R.; Huntsman, A. C.; Varikuti, S.; Oghumu, S.; Naman, C. B.; Pan, L.; Parinandi, N. L.; Papenfuss, T. L.; Kinghorn, A. D.; Bachelder, E. M.; Ainslie, K. M.; Fuchs, J. R.; Satoskar, A. R. Liposomal-encapsulated synthetic phytosterol protects against *Leishmania donovani* infection *in-vivo.* UNPUBLISHED WORKS

[16] Sharma, M.; Sehgal, R.; Kaur, S. Evaluation of Nephroprotective and Immunomodulatory Activities of Antioxidants in Combination with Cisplatin against Murine Visceral Leishmaniasis. *PLoS Neglected Tropical Diseases* **2012**, *6(5)*: e1629.

[17] Wege, A. K.; Florian, C.; Ernst, W.; Zimara, N.; Schleicher, U.; Hanses, F.; Schmid, M.; Ritter, U. *Leishmania major* Infection in Humanized Mice Induces Systemic Infection and Provokes a Nonprotective Human Immune Response. *PLoS neglected tropical diseases* **2012**, *6(7)*: e1741.

[18] Stäger, S.; Alexander, J.; Carter, K. C.; Brombacher, F.; Kaye, P. M. Both Interleukin-4 (IL-4) and IL-4 Receptor α Signaling Contribute to the Development of Hepatic Granulomas with Optimal Antileishmanial Activity. *Infect Immun* **2003**, *71(8)*, 4804-4807.

[19] Squires, K. E.; Schreiber, R. D.; McElrath, M. J.; Rubin, B. Y.; Anderson, S. L.; Murray, H. W. Experimental Visceral Leishmaniasis: Role of Endogenous IFN-γ in Host Defense and Tissue Granulomatous Response. *J Immunol* **1989**, *143(12)*, 4244-4249.

[20] Satoskar, A. R.; Rodig, S.; Telford, S. R.; Satoskar, A. A.; Ghosh, S. K.; Lichtenberg, F.; David, J. R. IL-12 gene-deficient C57BL/6 mice are susceptible to *Leishmania donovani* but have diminished hepatic immunopathology. *Eur J Immunol* **2000**, *30(3)*, 834-839.

[21] Murray, H. W. Endogenous Interleukin-12 Regulates Acquired Resistance in Experimental Visceral Leishmaniasis. *J Infect Dis* **1997**, *175(6)*, 1477-1479.

[22] Barton, D. H. R.; Wozniak, J.; Zard, S. Z. A Short and Efficient Degradation of the Bile Acid Side Chain: Some Novel Reactions of Sulphines and α-Ketoesters. *Tetrahedron* **1989**, *45(12)*, 3741-3754.

[23] Geoffroy, P.; Ressault, B.; Marchioni, E.; Miesch, M. Synthesis of Hoodigogenin A, aglycone of natural appetite suppressant glycosteroids extracted from *Hoodia gordonii*. *Steroids* **2011**, *76(7)*, 702-708.

[24] Woodard, J. L.; Abdelhamid, D. A. S. UNPUBLISHED WORKS

[25] Zhang, D. H.; Cai, F.; Zhou, X. D.; Zhou, W. S. A Concise and Stereoselective Synthesis of Squalamine. *Org. Lett.* **2003**, *5(18)*, 3257-3259.

[26] O'Doherty, G. A.; Li, H.; Bajaj, S. O.; Wang, H. Y. L.; Cuccarese, M. F.; Boger, R. Glycosylated Cardiotonic Steroids. WO 194068 A1, December 4, 2014.

[27] Li, Q.; Tochtrop, G. P. A stereoselective synthesis of the allo-bile acids from the 5β-isomers. *Tetrahedron Letters* **2011**, *52(32)*, 4137–4139.

[28] Mehvar, R.; Shepard, T. L.; Molecular-Weight-Dependent Pharmacokinetics of Fluorescein-Labeled Dextrans in Rats. *J. Pharm. Sci.* **1992**, *81(9)*, 908-912.

[29] Mehvar, R.; Robinson, M. A.; Reynolds, J. M. Molecular Weight Dependent Tissue Accumulation of Dextrans: *In Vivo* Studies in Rats. *J. Pharm. Sci.* **1994**, *83(10)*, 1495-1499.

[30] Zhang, X.; Mehvar, R. Dextran-Methylprednisolone Succinate as a Prodrug of Methylprednisolone: Plasma and Tissue Disposition. *J. Pharm. Sci.* **2001**, *90(12)*, 2078-2087.

[31] Mehvar, R. Simultaneous analysis of dextran-methylprednisolone succinate, methylprednisolone succinate, and methylprednisolone by size-exclusion chromatography. *Journal of Pharmaceutical and Biomedical Analysis* **1999**, *19(5)*, 785–792.

[32] McLeod, A. D.; Friend, D. R.; Tozer, T. N. Synthesis and chemical stability of glucocorticoid-dextran esters: potential prodrugs for colon-specific delivery. *Int. J. Pharmaceut.* **1993**, *92*, 105–114

[33] Hubel, K.; LeBmann, T.; Waldmann, H. Chemical biology – identification of small molecule modulators of cellular activity by natural product inspired synthesis. *Chem. Soc. Rev.* **2008**, *37(7)*, 1361–1374.

[34] McFedries, A.; Schwaid, A.; Saghatelian, A. Methods for the Elucidation of Protein-Small Molecule Interactions. *Chemistry & Biology* **2013**, *20*, 667-673.

[35] Ong, S.-E.; Blagoev, B.; Kratchmarova, I.; Kristensen, D. B.; Steen, H.; Pandey, A.; and Mann, M. Stable Isotope Labeling by Amino Acids in Cell Culture, SILAC, as a Simple and Accurate Approach to Expression Proteomics. *Molecular & Cellular Proteomics* **2002**, *1(5)*, 376–386.

[36] Ong, S.-E.; Schenone, M.; Margolin, A. A.; Li, X.; Do, K.; Doud, M. K.; Mani, D. R.; Kuai,

L.; Wang, X., Wood, J. L. *et al.* Identifying the proteins to which small-molecule probes and drugs bind in cells. *Proc. Natl. Acad. Sci. USA* **2009**, *106(12)*, 4617–4622.

[37] La Clair, J. J. *et al.* A Central Strategy for Converting Natural Products into Fluorescent Probes. *ChemBioChem* **2006**, *7(3)*, 409-416.

[38] Dey, B. B. A Study in the Coumarin Condensation. *J. Chem. Soc.* **1915**, *107*, 1606-1651.

Appendix: Characterization Data of Selected Compounds

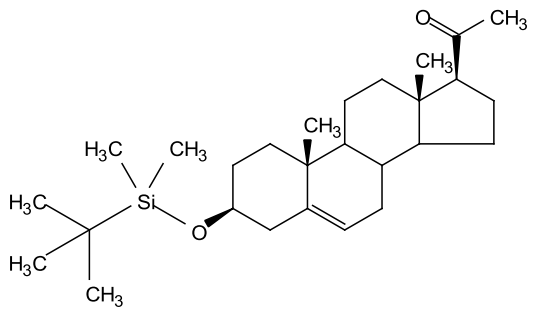

^{1}H NMR (400 MHz, $CDCl_3$)

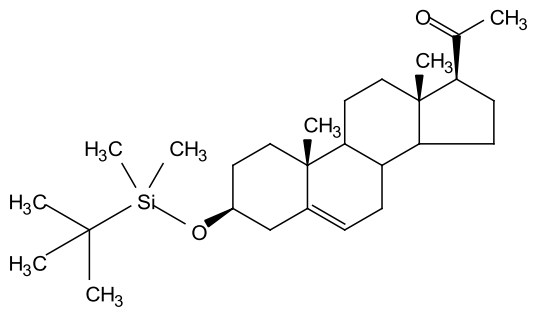

^{13}C NMR (100 MHz, $CDCl_3$)

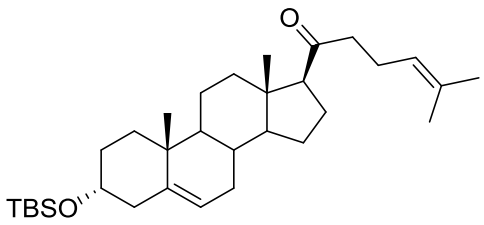

^{1}H NMR (300 MHz, $CDCl_3$)

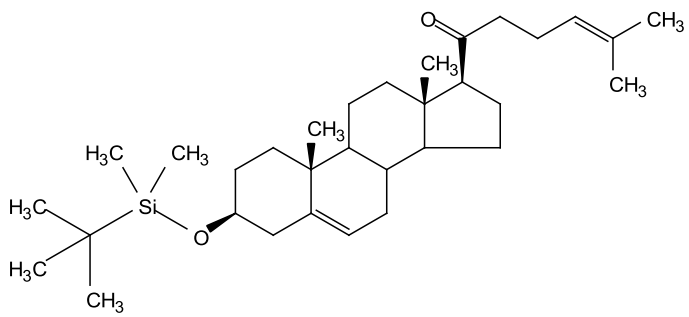

^{13}C NMR (100 MHz, $CDCl_3$)

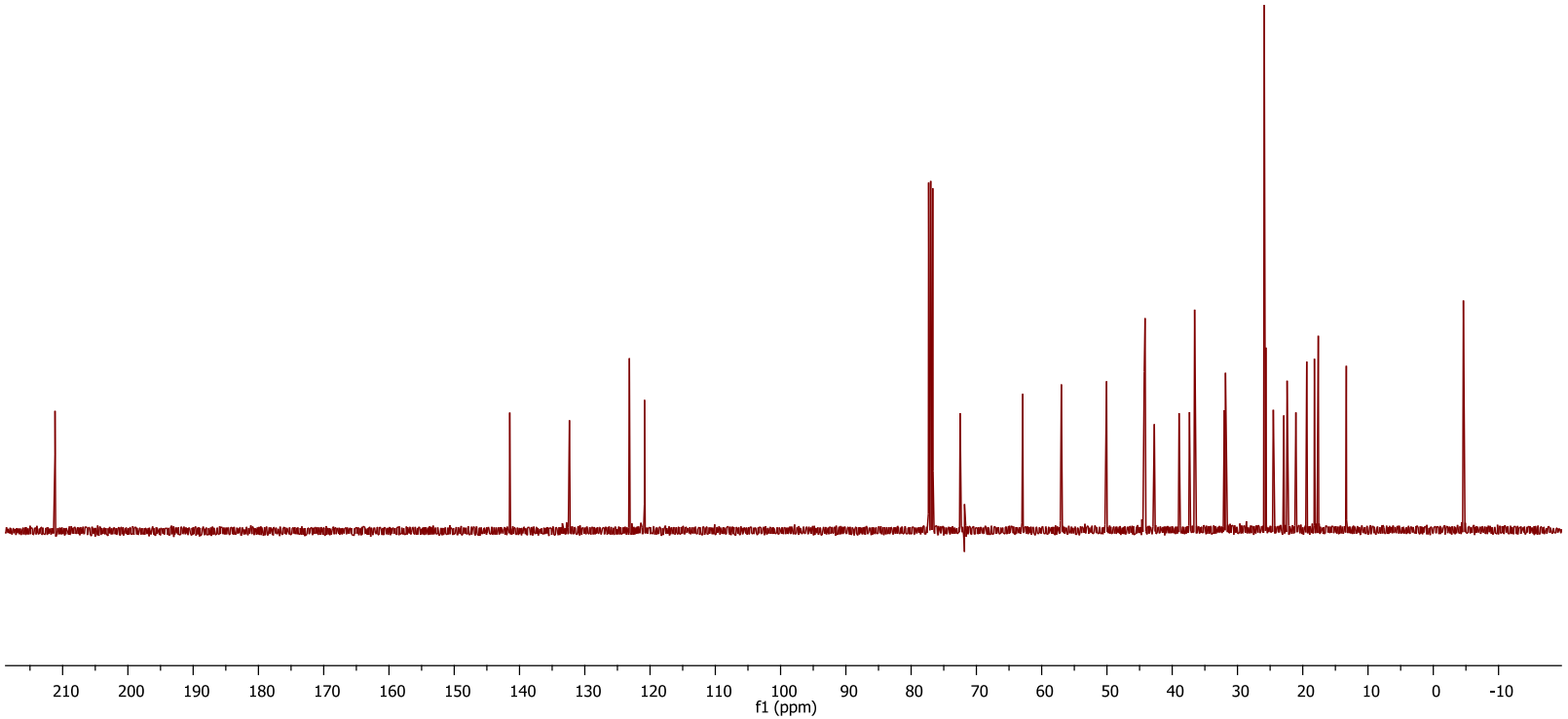

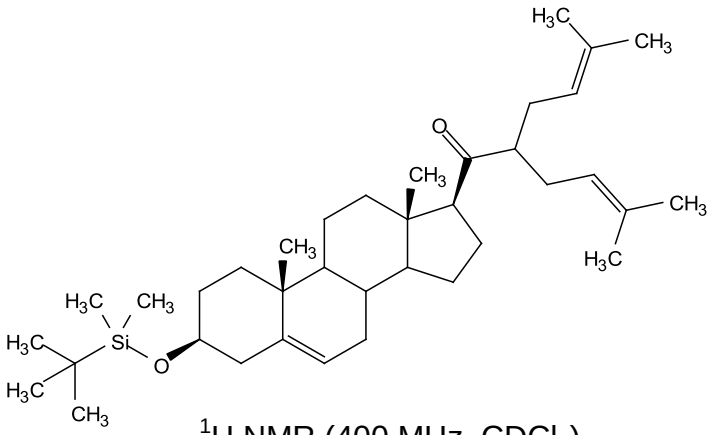

^{1}H NMR (400 MHz, $CDCl_3$)

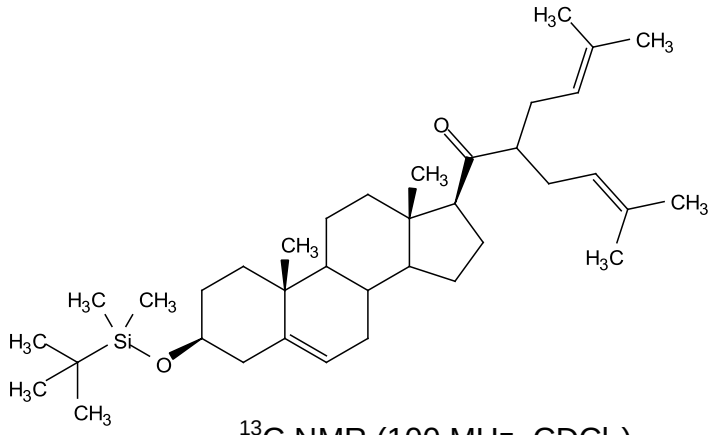

^{13}C NMR (100 MHz, $CDCl_3$)

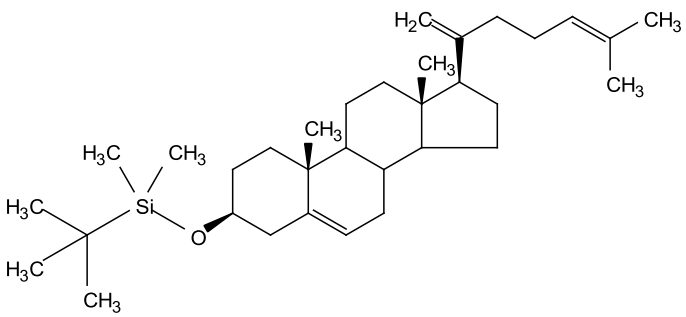

^{1}H NMR (400 MHz, $CDCl_3$)

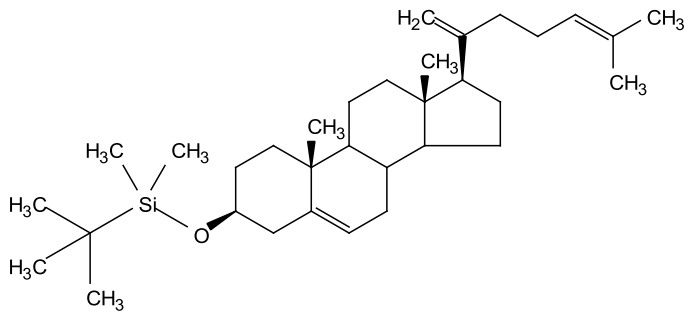

^{13}C NMR (100 MHz, $CDCl_3$)

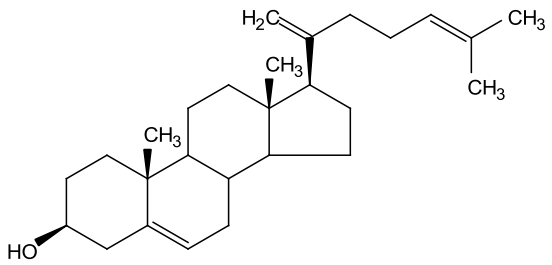

^{1}H NMR (400 MHz, $CDCl_3$)

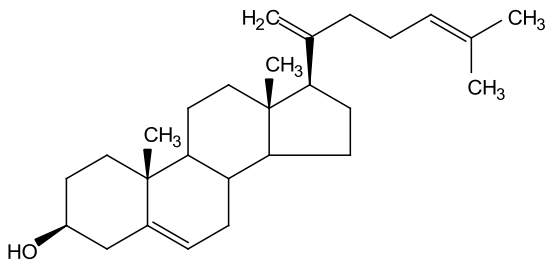

^{13}C NMR (100 MHz, $CDCl_3$)

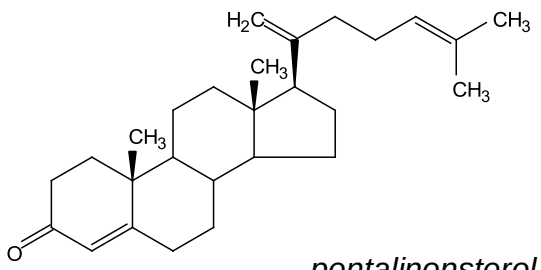

pentalinonsterol

^{1}H NMR (400 MHz, $CDCl_3$)

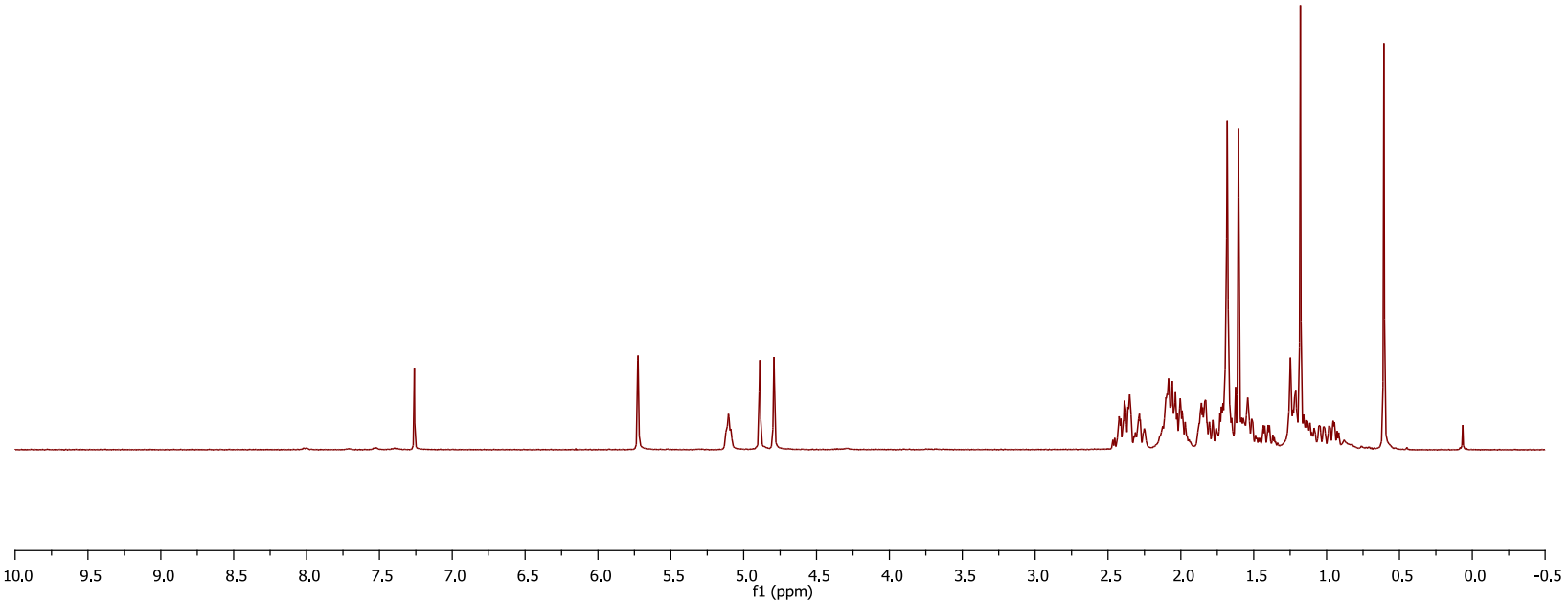

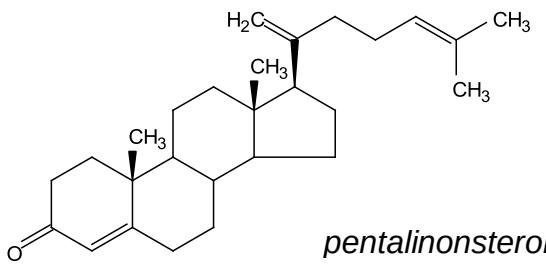

pentalinonsterol

^{13}C NMR (100 MHz, $CDCl_3$)

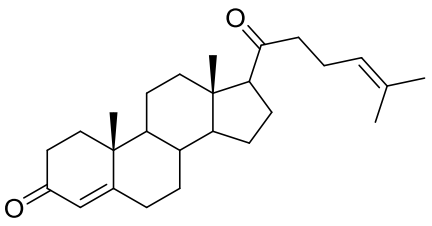

^{1}H NMR (300 MHz, $CDCl_3$)

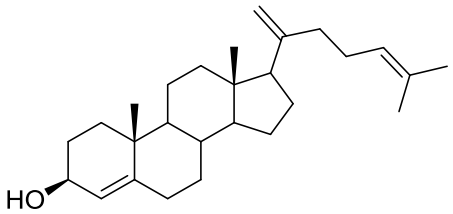

^{1}H NMR (400 MHz, $CDCl_3$)

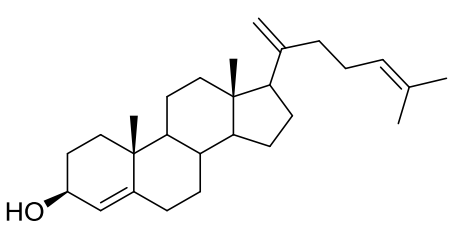

^{13}C NMR (100 MHz, $CDCl_3$)

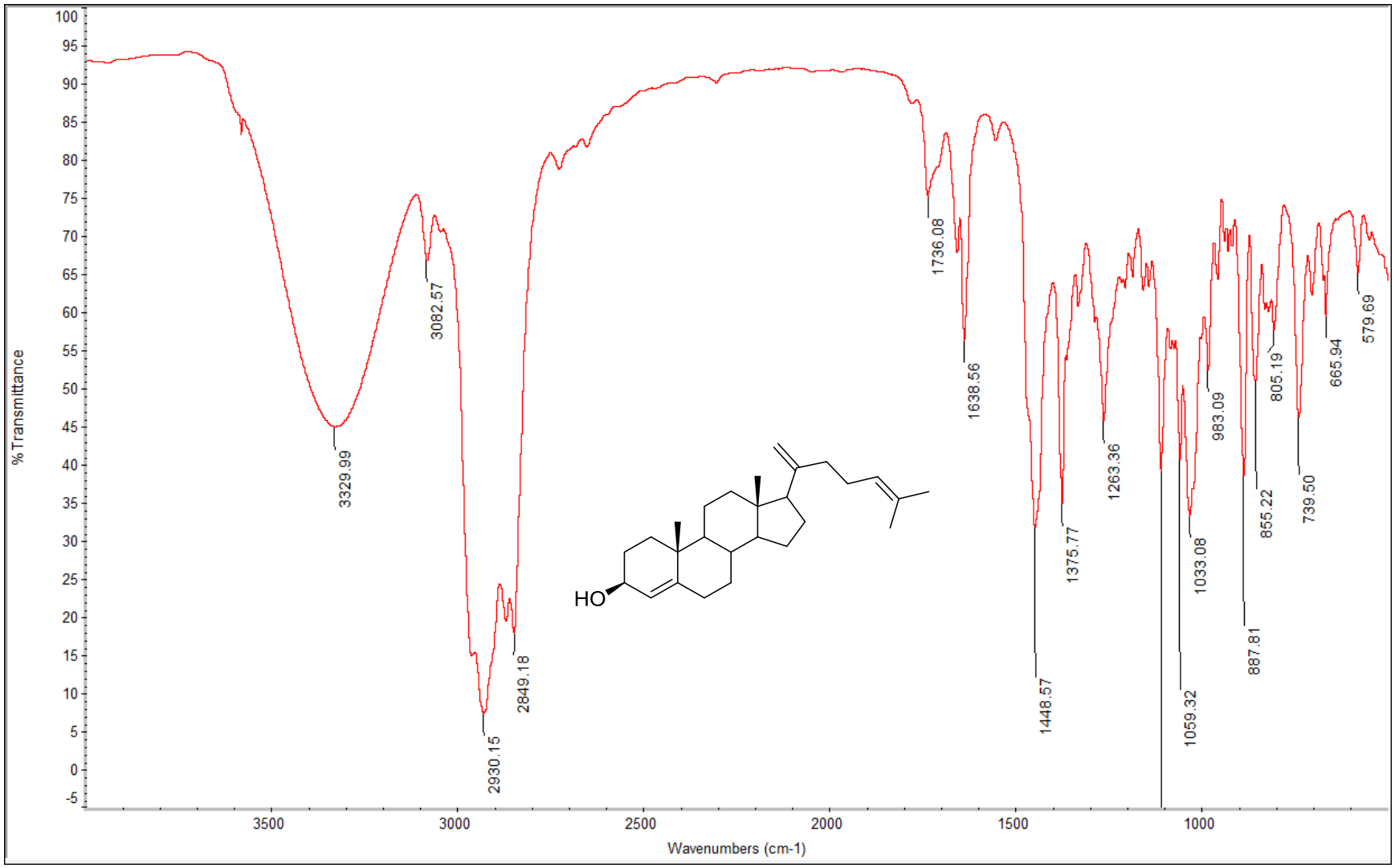
%Transmittance
Wavenumbers (cm-1)
3329.99
3082.57
2930.15
2849.18
1736.08
1638.56
1448.57
1375.77
1263.36
1059.32
1033.08
983.09
887.81
855.22
805.19
739.50
665.94
579.69
HO

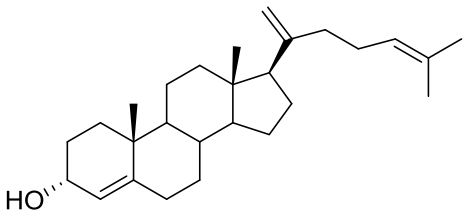

^{1}H NMR (250 MHz, $CDCl_3$)

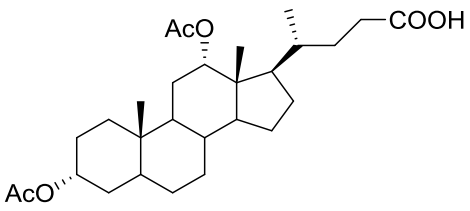

^{1}H NMR (400 MHz, $CDCl_3$)

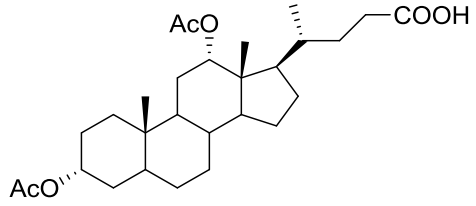

^{1}H NMR (100 MHz, $CDCl_3$)

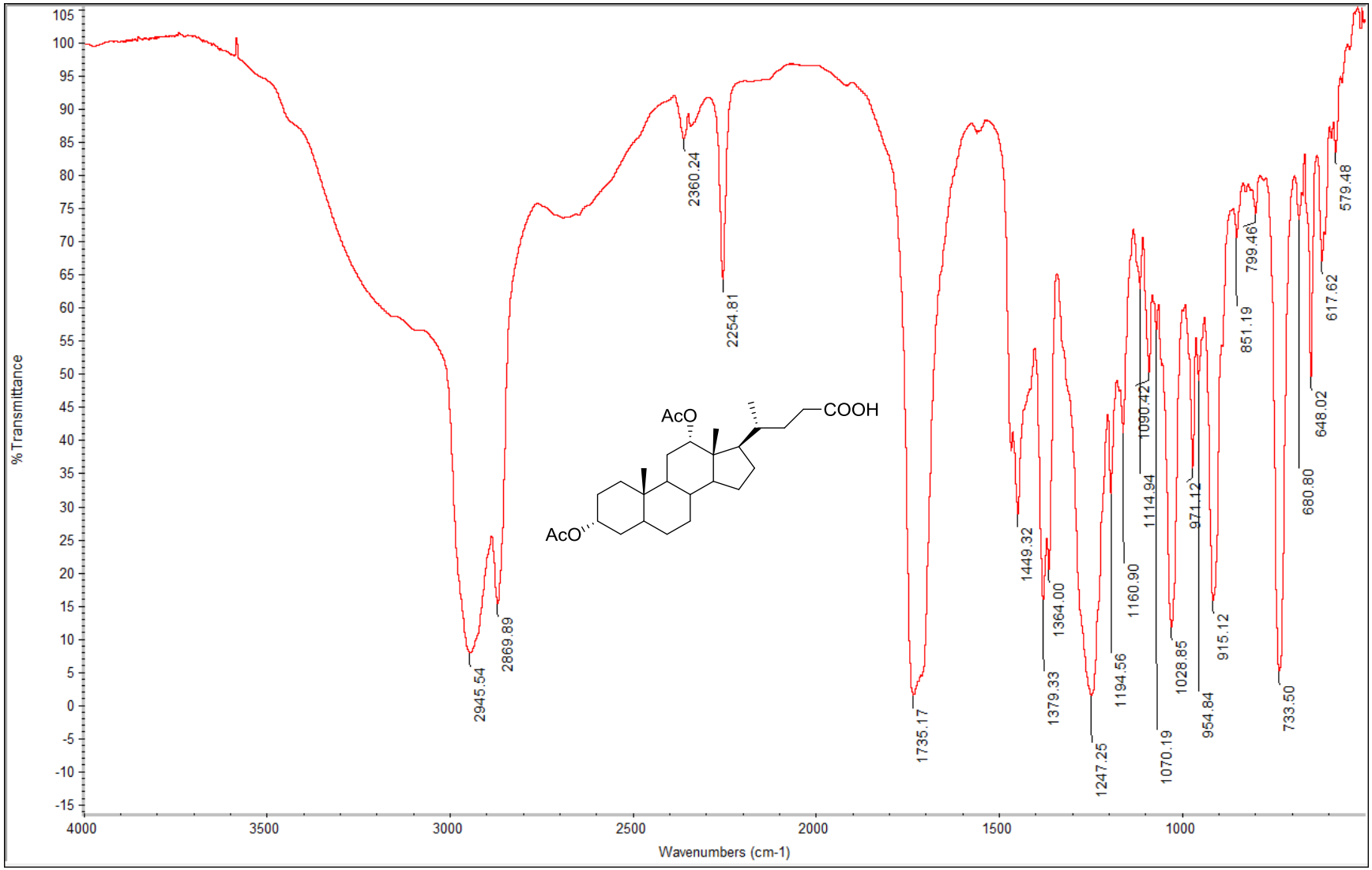
% Transmittance
Wavenumbers (cm-1)
2945.54
2869.89
2360.24
2254.81
1735.17
1449.32
1379.33
1364.00
1247.25
1194.56
1160.90
1114.94
1090.42
1070.19
1028.85
971.12
954.84
915.12
851.19
799.46
733.50
680.80
648.02
617.62
579.48
AcO
AcO
COOH

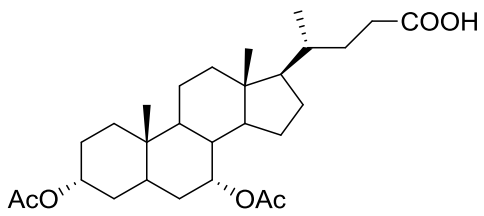

^{1}H NMR (400 MHz, $CDCl_3$)

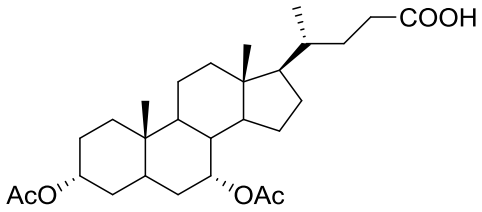

^{1}H NMR (100 MHz, $CDCl_3$)

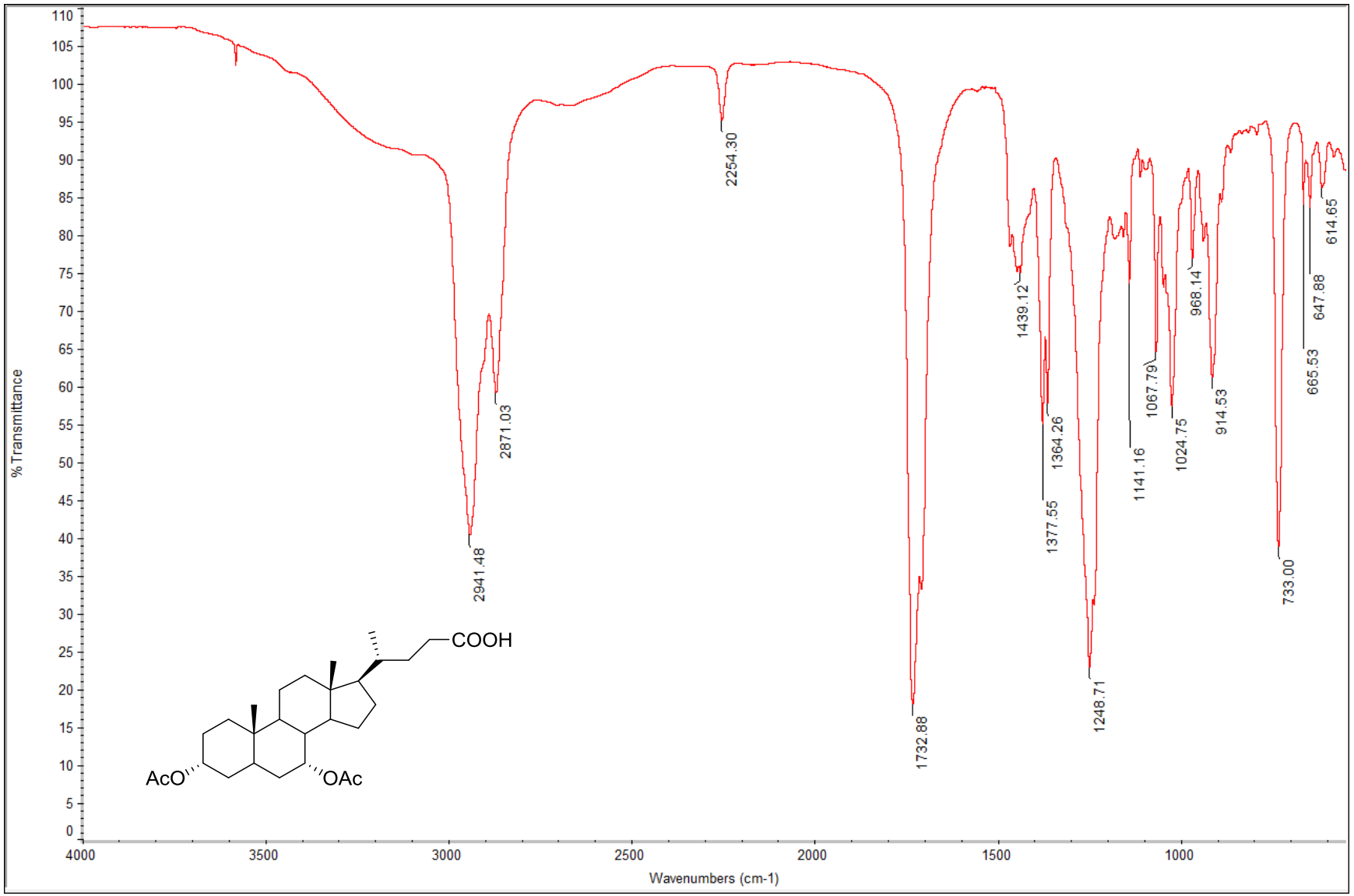
% Transmittance
Wavenumbers (cm-1)
2941.48
2871.03
2254.30
1732.88
1439.12
1377.55
1364.26
1248.71
1141.16
1067.79
1024.75
968.14
914.53
733.00
665.53
647.88
614.65
COOH
AcO
OAc

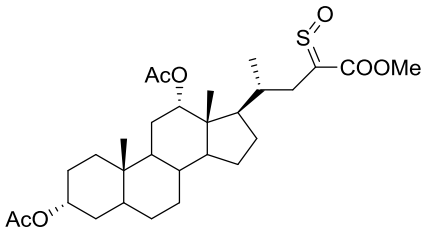

^{1}H NMR (400 MHz, $CDCl_3$)

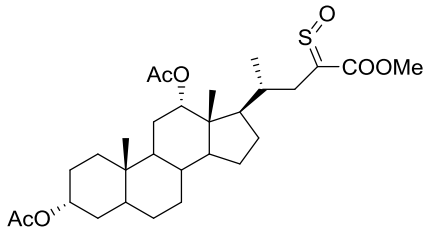

^{1}H NMR (100 MHz, $CDCl_3$)

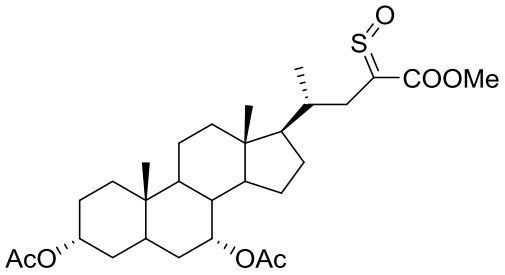

^{1}H NMR (400 MHz, $CDCl_3$)

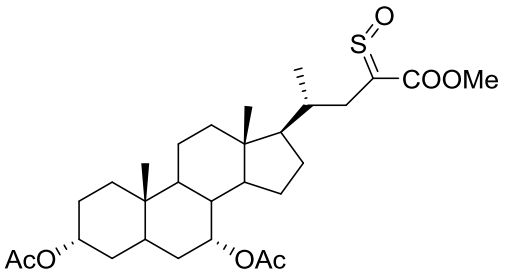

^{1}H NMR (100 MHz, $CDCl_3$)

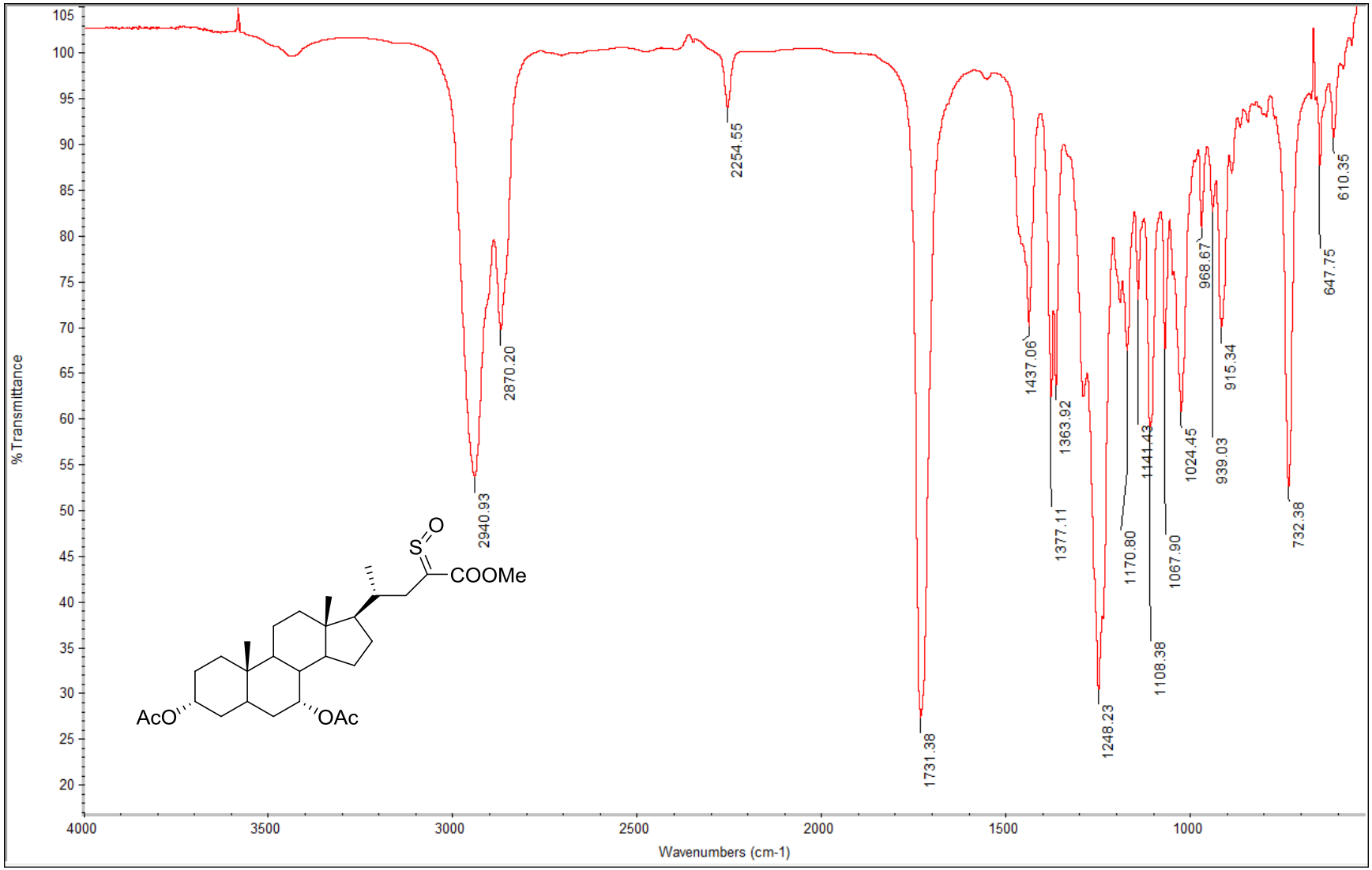
% Transmittance
Wavenumbers (cm-1)
2940.93
2870.20
2254.55
1731.38
1437.06
1377.11
1363.92
1248.23
1170.80
1141.43
1108.38
1067.90
1024.45
968.67
939.03
915.34
732.38
647.75
610.35
S
O
COOMe
AcO
OAc

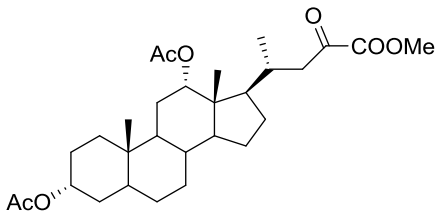

^{1}H NMR (400 MHz, $CDCl_3$)

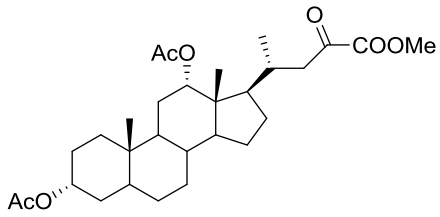

^{1}H NMR (100 MHz, $CDCl_3$)

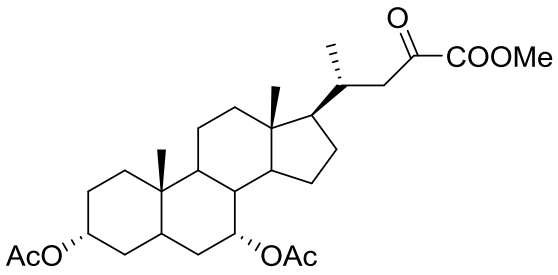

^{1}H NMR (400 MHz, $CDCl_3$)

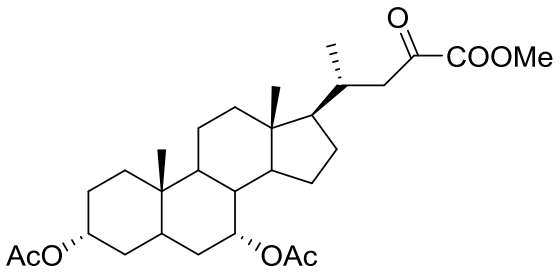

^{1}H NMR (100 MHz, $CDCl_3$)

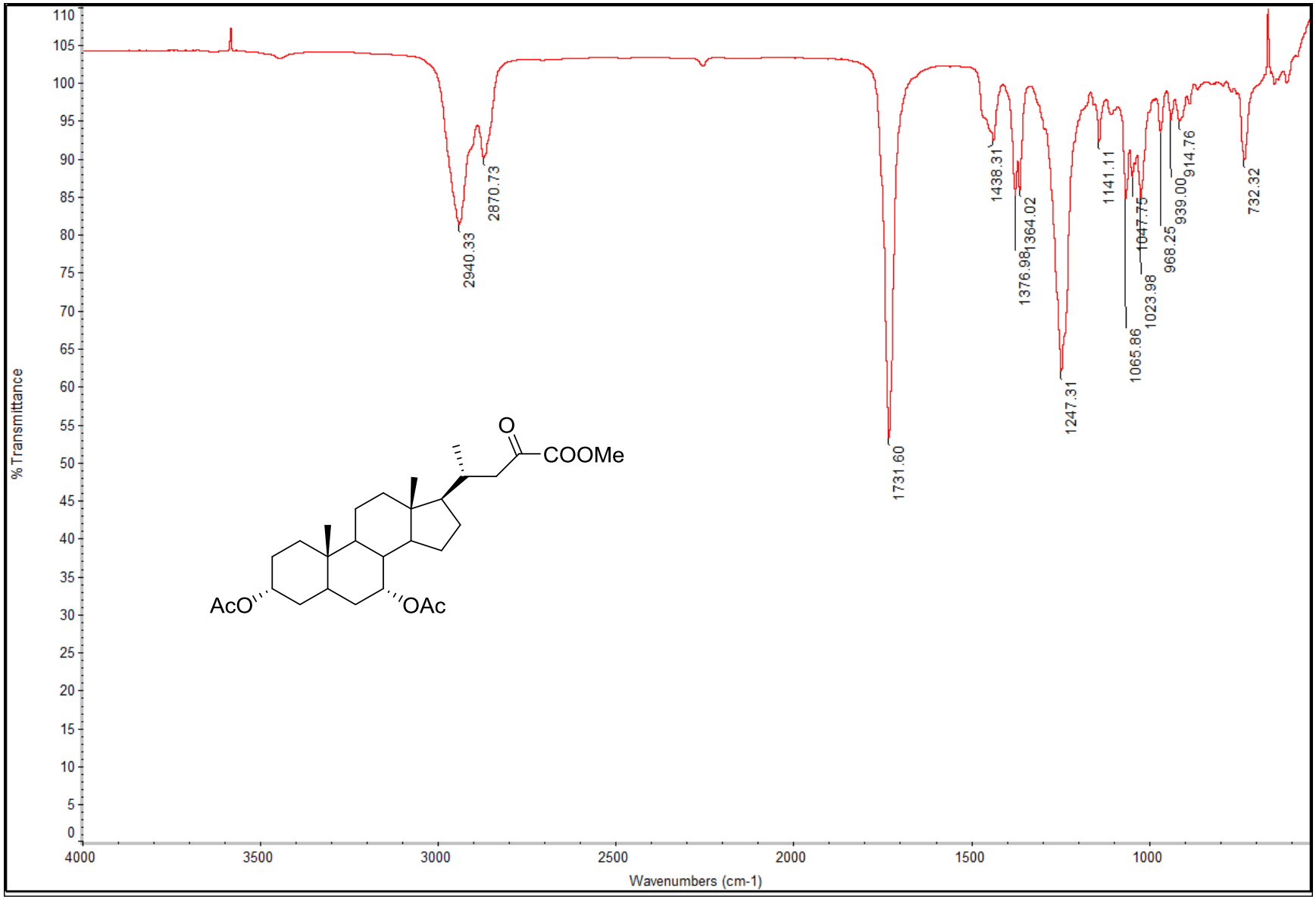
% Transmittance
Wavenumbers (cm-1)
2940.33
2870.73
1731.60
1438.31
1376.98
1364.02
1247.31
1141.11
1065.86
1047.75
1023.98
968.25
939.00
914.76
732.32
O
COOMe
AcO
OAc

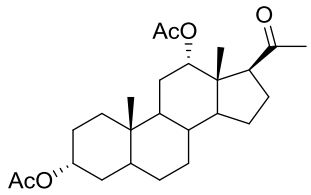

^{1}H NMR (400 MHz, $CDCl_3$)

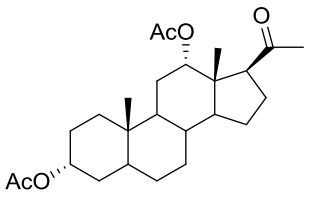

^{1}H NMR (100 MHz, $CDCl_3$)

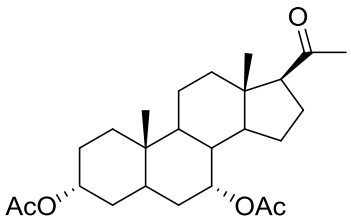

^{1}H NMR (400 MHz, $CDCl_3$)

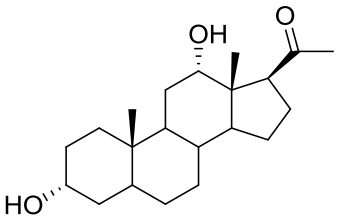

^{1}H NMR (300 MHz, $CDCl_3$)

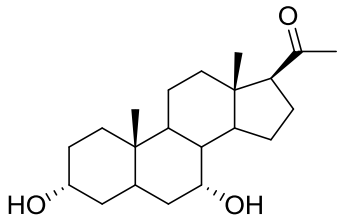

^{1}H NMR (300 MHz, $CDCl_3$)

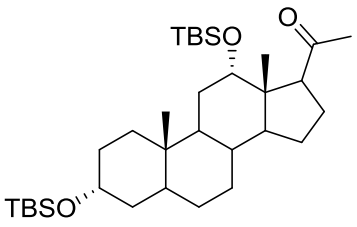

^{1}H NMR (400 MHz, $CDCl_3$)

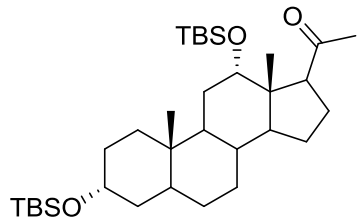

^{13}C NMR (100 MHz, $CDCl_3$)

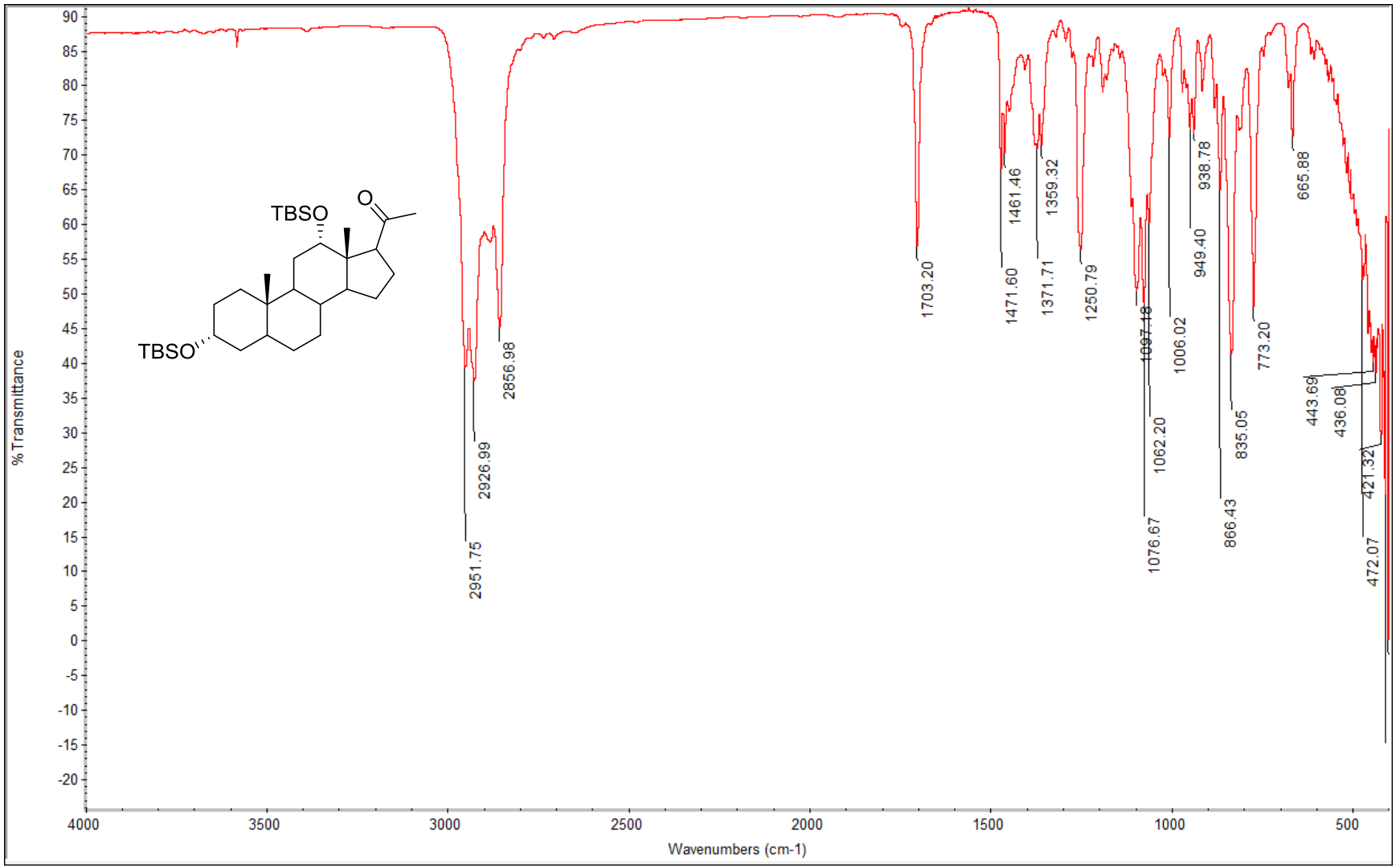
TBSO
O
TBSO
% Transmittance
Wavenumbers (cm-1)
2951.75
2926.99
2856.98
1703.20
1471.60
1461.46
1371.71
1359.32
1250.79
1097.18
1076.67
1062.20
1006.02
949.40
938.78
866.43
835.05
773.20
665.88
472.07
443.69
436.08
421.32

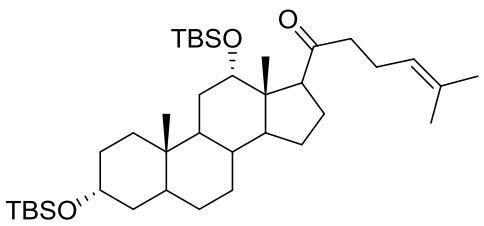

^{1}H NMR (400 MHz, $CDCl_3$)

END